

INVESTIGATION OF DISTRIBUTION SYSTEM MESHED CONFIGURATION TO  
INCREASE MAXIMUM ALLOWABLE PENETRATION OF  
DISTRIBUTED GENERATION

by

Masoud Davoudi

A thesis submitted to the faculty of  
The University of North Carolina at Charlotte  
in partial fulfillment of the requirements  
for the degree of Master of Science in  
Electrical Engineering

Charlotte

2014

Approved by:

---

Dr. Valentina Cecchi

---

Dr. Mehdi Miri

---

Dr. Zia Salami



## ABSTRACT

MASOUD DAVOUDI. Investigation of distribution system meshed configuration to increase maximum allowable penetration of distributed generation. (Under the direction of DR. VALENTINA CECCHI)

Electrical distribution systems have been traditionally planned and operated in a radial manner, allowing uni-directional flow of power from substation to customers. In recent years, environmental and societal concerns have prompted an increased use of renewable Distributed Generation (DG) connected to the distribution system. The proliferation of DG impacts both system operation and planning. Robust long term solutions are then needed to overcome the physical limitations of the distribution system radial configuration for higher DG penetration levels.

This thesis evaluates meshed configuration as a possible solution to allow for higher penetration levels of DG. Steady-state bus voltages and line currents are selected as main limiting factors to increased DG penetration levels. Then, a method is presented to determine maximum allowable DG power injection at different buses in the system considering these limiting factors. The presented method can be used in both planning and operation scenarios, since it is fast and has low computational burden. Using this method, radial and meshed configurations of a distribution system are evaluated with respect to their ability to withstand higher DG penetration levels. The results of the study verify the superior behavior of select meshed configurations to accommodate proliferation of DG.

## ACKNOWLEDGMENTS

I would like to express the deepest appreciation to my advisor, Dr. Valentina Cecchi, for all her help in performing this research and developing this thesis. I thank her for her excellent guidance and caring, providing me with an excellent atmosphere for doing research, and sharing with me her passion for research. I would also like to thank Dr. Romero Agüero for his valuable insights and ideas in improving the work. I like to appreciate the committee members, Dr. Miri and Dr. Salami, for their insightful comments and for the time they dedicated to reviewing this work. I would like to acknowledge my wife, for her true love and standing by me through the good times and the difficulties, and my family, who has always supported me through my life. Finally, I would like to thank everyone who has helped me directly or indirectly in completing this work.

## TABLE OF CONTENTS

LIST OF TABLES	vii
LIST OF FIGURES	viii
CHAPTER 1: INTRODUCTION AND PROBLEM STATEMENT	1
1.1 Overview	1
1.2 Background and Motivation	2
1.3 Electric Power Distribution Systems	3
1.4 Distributed Generation (DG)	7
1.5 Prior Work	10
1.6 Problem Statement	11
1.7 Organization of Thesis	14
CHAPTER 2: METHODS TO DETERMINE MAXIMUM ALLOWABLE DG INJECTION	15
2.1 Overview	15
2.2 Repetitive Power Flow Method	16
2.3 Proposed Method for Determining Maximum Allowable DG Injection Based on Steady State Voltage and Current Limits	18
2.3.1 Considering Bus Voltages	19
2.3.2 Considering Line Currents	23
CHAPTER 3: EFFECTS OF CHANGING DISTRIBUTION SYSTEM CONFIGURATION	28
3.1 Overview	28
3.2 Expected Changes in DG Maximum Allowable Power Injection	28

CHAPTER 4: ASSESSMENT OF DISTRIBUTION SYSTEM MESHED CONFIGURATION FOR INCREASED DG PENETRATION: A CASE STUDY	34
4.1 Overview	34
4.2 System Specification: 69 Bus Test System	35
4.3 Effect of System Configuration: Radial vs. Meshed	40
4.3.1 Expected Changes Due to Different Configuration: An Example	40
4.3.2 Maximum Demand Scenario	46
4.3.3 Minimum Demand Scenario	50
4.4 Effect of DG Power Factor	54
4.5 Multiple DG Cases: Effect of Radial vs. Meshed Configuration	60
4.6 Summary of Results and Observations	63
CHAPTER 5: CONCLUSION	66
5.1 Overview	66
5.2 Summary of Research Contributions	66
5.3 Future Work and Vision	68
REFERENCES	70

## LIST OF TABLES

TABLE 4.1: Load data for the maximum demand scenario	37
TABLE 4.2: Line data for the test case	38
TABLE 4.3: Calculating $P_{27}^{Max,27}$ for different configurations	43
TABLE 4.4: Max. allowable power injection in end-lateral buses in case of having a DG located at bus 65 generating 1 MW	61
TABLE 4.5: Max. allowable power injection in end-lateral buses in case of having a DG located at bus 65 generating 1.871 MW ( $P_{65}^{Max,Total}$ )	61
TABLE 4.6: Max. allowable power injection in end-lateral buses in case of having a DG located at bus 65 and 27, each generating 1.87 MW and 0.69 MW, respectively	62
TABLE 4.7: Average max. allowable power injection in the system for different configurations and DG power factors in maximum demand scenario	63
TABLE 4.8: Active and reactive power losses in the system in each configuration	65

## LIST OF FIGURES

FIGURE 1.1: Different sections of a typical electrical power system	4
FIGURE 1.2: Different parts of a typical distribution system	5
FIGURE 2.1: Repetitive power flow method for determining maximum allowable power injection at a bus	17
FIGURE 2.2: Flowchart for determining maximum allowable DG injection based on voltage limits and DG capacity	23
FIGURE 2.3: Determining the maximum allowable generation of a DG	25
FIGURE 4.1: Test case system	35
FIGURE 4.2: Bus voltages in different system configurations in maximum demand scenario without DG	41
FIGURE 4.3: Bus voltages for different power injections at bus 27 in a) radial case and b) meshed case $C_2$	45
FIGURE 4.4: $P^{Max,Total}$ for all system buses in different system configurations, maximum demand scenario and DG unity power factor	49
FIGURE 4.5: $P^{Max,Total}$ for end-lateral buses in different configurations in maximum demand scenario	50
FIGURE 4.6: System voltage profile for radial configuration without DG in maximum and minimum demand scenario	51
FIGURE 4.7: $P^{Max,Total}$ for all system buses in different system configurations, minimum demand scenario and DG unity power factor	52
FIGURE 4.8: $P^{Max,Total}$ in different system configurations in DG unity power factor in minimum and maximum demand scenarios	53
FIGURE 4.9: $P^{Max,V,DG}$ and $P^{Max,Total}$ in radial configuration and maximum demand scenario for different DG power factors	55
FIGURE 4.10: $P^{Max,Total}$ in maximum demand scenario for different system configuration in a) 0.9 and b) 0.8 capacitive mode of DG operation	58



- FIGURE 4.11:  $P^{Max,Total}$  in maximum demand scenario for different system configurations in a) 0.9 and b) 0.8 inductive mode of DG operation 59
- FIGURE 4.12: Average  $P^{Max,Total}$  (MW) for different configurations and DG power factors in in maximum demand scenario 64

## CHAPTER 1: INTRODUCTION AND PROBLEM STATEMENT

### 1.1 Overview

Use of Distributed Generation (DG) in the electric power Distribution System (DS) provides the opportunity to improve system efficiency and reliability by supplying power locally. In recent years, societal and environmental concerns have led to a push toward proliferation of DG and mainly renewable DG in the system. However, distribution systems are traditionally planned and operated based on the hypothesis of uni-directional flow of power from the substation to the loads, and some parts of the DS might need reinforcements in high penetration levels of DG. Therefore, there is a need to accommodate growing penetration levels of DG, including photovoltaic and plug-in electric vehicles. The advent of smart system technologies and advances in protection systems and distribution automation provide motivation to consider alternative modes of operating the DS. Specifically, meshed distribution systems may be considered an appropriate solution for maximizing system's ability to integrate large amounts of renewable and distributed generation.

This thesis concentrates on evaluating meshed operation of DS with respect to allowing more penetration levels of distributed generation. In this chapter, the following topics are presented:

- A background and motivation for the work;
- A brief review of electric power distribution systems and distributed generation;

- A brief review of electric power distribution systems and distributed generation;
- A review of selected prior work;
- A problem statement; and
- An overview of the thesis organization.

## 1.2 Background and Motivation

Electric power distribution systems are traditionally operated in a radial manner, allowing the power to flow from the only source of power (substation) toward the loads distributed along the laterals. With the advent of power electronics technology and use of renewable energies, distribution systems are under an unprecedented evolution driven by the proliferation of DG. Optimal or adequate injections of DG introduce several advantages, like improving the voltage profile and reducing losses. However, with the presence of DG in the DS, the assumption of uni-directional flow of power in the system is not valid anymore. This will affect the operation of voltage regulators and of the protection system (e.g. increased short circuit currents and mis-coordination). Moreover, steady state voltage rises might occur in case of increased injection levels of DG. Line currents in the system might also increase when connecting a DG to the system. Intermittency and variable output of the DG may also cause voltage flickers.

These effects have impacted distribution systems planning and operation. Part of the solution to allow high penetration levels of DG could include robust real-time control which helps operate this highly dynamic system maintaining quality, reliability, efficiency and security expectations. However, control-based solutions do not overcome the physical limitations of the distribution system radial configuration such as feeder capacity. Therefore, injecting higher levels of power (from DG) into the system requires

alternative operation modes of distribution feeders. Closed-loop operation of distribution system has shown to have various advantages to the conventional radial operation, such as decreased power losses and improved voltage profile. This configuration can present a promissory solution for maximizing system's ability to integrate larger amounts of renewable generation.

In this thesis, closed-form equations are used to determine the maximum allowable power injection at different system buses. Using this method, radial and meshed configurations of a distribution system are compared with respect to their ability to withstand higher penetration levels of DG. The results of the study verify the superior behavior of meshed configurations to accommodate proliferation of DG.

### 1.3 Electric Power Distribution Systems

Electric power systems consist of different parts, namely generation, transmission, and distribution, with specific task dedicated to each of them [1][2]. Figure 1.1 shows a schematic of power system with its subsections. Traditionally, electric power is generated from bulk power plants at voltage levels around 11 kV to 25 kV. Then, this power is converted to a higher voltage level, typically higher than 120 kV, to be transmitted with the transmission system. Then, the sub-transmission system carries the power to the distribution system, which is typically of voltages lower than 69 kV. The distribution system is the final stage in the process of delivering power from generation to the end users and is the system closest to the customers.

Figure 1.2 shows a typical distribution system. Distribution systems usually start at the distribution substation, which lowers the voltage level of the power delivered by a sub-transmission line, or directly by a transmission line. The existence of sub-

transmission system depends on the area that the distribution system covers, since if the loads are concentrated in different places far from each other, using a sub-transmission system is helpful to deliver the power to the bulk area of the load and then convert it to a lower voltage level, where the distribution system starts functioning. If the load is diverse, lower voltage level might be needed from the beginning and hence distribution system with its lower voltage level starts delivering the power immediately after the transmission system. This also depends on the utility company [2].

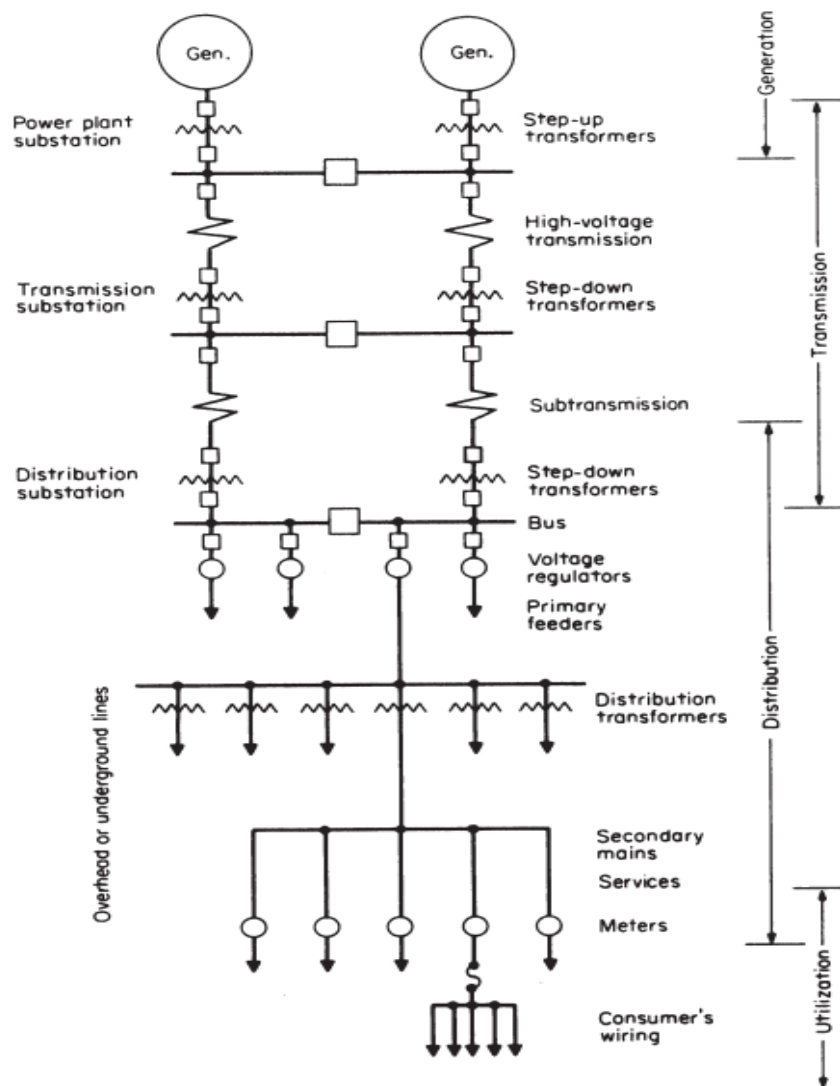


Figure 1.1: Different sections of a typical electrical power system [2]

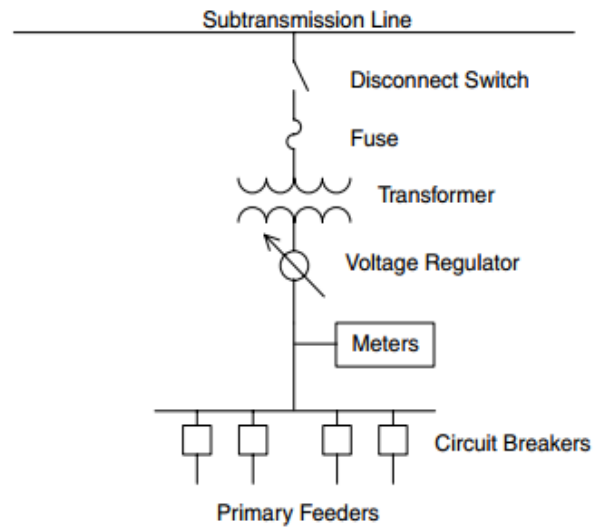


Figure 1.2: Different parts of a typical distribution system [1]

A typical distribution system consists of one or more distribution substations. Each distribution substation feeds one or more primary feeder(s). The primary feeder then delivers the power to the secondary systems through a step-down distribution transformer, which will deliver the power to the end users.

In the last few decades, power plants have become larger and their generation levels have increased. Transmission systems have also been highly developed and expanded geographically to deliver power to more areas in the nation. However, distribution systems have been referred to as the “unglamorous” [1] part of the power system and their importance has been traditionally undervalued. The loads in a distribution system are usually distributed, which makes the analysis of distribution system more complicated than the transmission system with concentrated loads. Moreover, distribution systems may have one, two and three phase lines as well as underground cables, while transmission systems are usually three phase. Distribution systems are inherently unbalanced, typically due to the unbalanced loads in different

phases, unbalanced line impedances in the distribution system, and also having one, two, or three phase section. This leads to a typical voltage unbalance of 5% to 30% in distribution systems in comparison to a typical unbalance of below 5% in transmission systems. The number of components in a distribution system is almost 100 times more than the transmission system, and its capital outlay is almost 40% of the total power system, which is almost twice that of the transmission system.

Historically, especially in the United States, suburban and rural distribution systems have been designed and operated in a radial manner, which are characterized by unidirectional flow of power from the substation to each customer. Radial configuration has been predominant due to its simple and economical operation and protection requirements. However, this configuration has evident efficiency and reliability shortcomings. A fault disconnection would discontinue the service to all downstream loads. Moreover, this configuration causes significant voltage drop along the feeder, and has higher power losses. In order to increase the reliability of radial configuration, normally open tie-switches and normally closed circuit breakers have been used. In case of a fault, these switches will change conditions and the continuity of service is held. This concept is referred to as reconfiguration, and can also be done to improve voltage profile, decrease power losses, and/or other benefits [3][4][5].

Nowadays, with the advent of smart system technologies and Distribution Automation (DA), more attention has been focused on intelligent power systems with the aim of increasing efficiency, stability, reliability and power quality. Smart system includes bi-directional flow of information and power, and decentralized supply and control, which will enable active participation by customers. Distribution Automation

(DA) refers to a system which allows for monitoring, control, and operating the distribution system remotely in a real time mode. With the increased presence of DG, traditionally passive distribution systems have changed to active elements of power systems, and as an important part of the power system, the operators are now more interested in controlling the behavior of the distribution system using for example distribution automation and demand side management.

Increased interest in renewable energy resources [6] has led to a need for operating the distribution system at its maximum available capacity. Advances in smart system technologies, DA, power electronics, and protection technologies have paved the way for exploring alternative distribution operation modes. One possible approach is forming loops in the primary distribution systems, similar to transmission lines, which is referred to as meshed configuration in this thesis. Despite its complexity and concerns, this mode of operating the distribution system has several benefits, which will be discussed in Section 1.5.

#### 1.4 Distributed Generation (DG)

Distributed generation refers to small power generation units usually connected at the distribution voltage levels which inject energy to the distribution system locally, in comparison with the bulk power plants that generate higher amounts of electrical power. Different reasons have led to introducing these new types of generation in the power system [6][7]. The first reason is deregulation of the electricity market, which enables the small sized generation units to play a role in the market, competing with the large sized substations. Another reason is environmental concerns. Conventional power plants use fossil fuels, which have prompted concerns about their carbon emissions. Nuclear and



hydro power plants, although not having carbon emissions, affect the environment in other ways. With the advances in power electronic technologies, integrating renewable energies to the system has become easier and in addition to utility-sized renewable DG units, small residential sized Photovoltaic (PV) systems are also commonly used nowadays. Moreover, generating power locally is more efficient in terms of system power losses, and may increase system reliability [3][8].

Different types of renewable energy as well as fossil fuels can be used as DG. The renewable DG refer to wind, solar, combined heat and power, hydropower, and other categories. Installing distributed-type generation (DG) in the distribution system can have positive and negative effects on the system, and there is a need to adequately choose the permissible amount of DG penetration such that the advantages are not turned into disadvantages.

Integrating DG in the network, if properly sized and located, can have advantages for the system. Regardless of its type, a DG may increase the reliability of power supply provided to the customers [9][10]. Another advantage of DG installation is the reduction in overall system losses [3][11]-[13], since the current through the main feeder from substation to the DG Point of Common Coupling (PCC) can generally be decreased. DG will also impact system planning, which could result in deferment of investment [7]. Since the power is locally generated, it will improve the voltage profile and power quality, which will enable the system to withstand higher demand levels [6]. Moreover, use of renewable DG contributes to the reduction of pollution and greenhouse gases.

On the other hand, DG may have some negative impacts on the system. Some renewable types of DG inject the power to the system using power electronic devices,

which in turn will increase the harmonic level in the system [14]-[17]. Moreover, if the DG location and size is not selected properly, injection of power from the DG might cause overvoltages [3][18][19]. Furthermore, it can even lead to higher power losses in the system [3]. Higher losses can occur when the reverse power flow through a branch after DG interconnection is increased more than its forward power flow prior to connecting the DG to the system. With respect to distribution system configuration, since distribution systems are typically operated radially, the power flow in the lines are uni-directional and the main protection devices are fuses or uni-directional current relays. The power injected by a DG, which is often connected towards the end of the feeder and laterals, may change the current direction in some lines. This may affect operation of voltage regulators, mainly designed for unidirectional systems. It will also require some updates in the protection system, by modifying relay settings and/or changing fuses to relays or unidirectional relays to bidirectional ones. Some other concerns are related to the intermittency and variability of renewable-type of generation (e.g. solar photovoltaic) or by undesired islanding of a DG [6][20]-[22]. Another impact is voltage fluctuations due to the intermittent nature of some types of DG, which can cause temporary overvoltages in the system [21].

As the interest to inject more renewable-type DG into the system is increasing, the concerns related to interconnections of DG are becoming increasingly more important. In general, the system, and all its elements, should be able to accommodate the desired level of DG penetration. Limiting factors to the increased penetration levels of DG include violations of bus voltage and line current limits, interaction with voltage regulators and control schemes, and effects on the correct operation of protection systems. Furthermore,

as the output of a DG is increased, the voltages in the system are generally boosted, which is preferred in the buses towards the end of laterals. However, the amount of voltage increase should not exceed the steady state limitations on the buses. If the DG absorbs reactive power, in some buses, the voltage might be decreased by increasing its penetration level, and the minimum steady state voltage limit should be considered. Moreover, by injecting power into the system, line currents will change, and the penetration level should not increase line currents above their loadability limit. With the advent of power electronics technology, the amount of harmonic injections from DG units has been significantly decreased [23]. However, some papers have considered DG harmonic injections as a limiting factor for increasing DG penetration [14][15].

### 1.5 Prior Work

Meshed configuration of the distribution system increases the complexity of planning and operating the network. For example, it requires updates to the protection system and results in additional costs to the system operators [24][25]. Meshed configuration also introduces several advantages [3][8][26]-[28], it has shown to improve system reliability, since it provides multiple paths for the power to flow to the end-lateral nodes [26]. In [26], an existing meshed distribution system has been compared with its previous radial configuration; the meshed configuration has shown superior behavior in terms of reliability, voltage profile, and exploitation level of transformers and lines. In [3], meshed configuration has been presented as a method to decrease power losses in the system, which also improves voltage profile. It has also been noted that the proper sizing and location of the DG helps to improve the efficiency of the meshed configuration in comparison with the radial case. The need to reinforce the existing radial feeders and the

possible solution of forming loops in the system has been presented in [8]. In [8], it is also noted that radial systems which have emergency tie-lines already have the possibility of being operated in meshed configuration, and meshed configuration does not require building new lines. Moreover, the paper shows that meshed operation helps to prevent overloading of transformers and lines. In [18] and [27][28], meshed configuration has shown better voltage profile in case of having DG in the system in comparison with the radial case.

Different methods to determine the maximum allowable DG penetration level have been proposed in the literature. In [29] and [30], the maximum allowable DG injection is determined based on steady state voltage limits. In [14] and [15], harmonic distortion levels are used to determine the maximum allowable DG output in the system. In [31], a method has been presented to determine the allowable DG injection before the coordination between over current relays is violated. In general, the aim has been on increasing the penetration level of DG in the distribution system using power electronic devices or energy storage systems [32], or by controlling the reactive power consumption of the DG [19].

With careful planning, meshed operation of the distribution system could be such that the negative impacts of meshed operation are omitted or decreased, and the positive effects could be exploited [8][26]. Hence, distribution system meshed configuration can be selected as a robust solution for increasing the ability of distribution systems to withstand higher injections of renewable and distributed generation.

## 1.6 Problem Statement

With the increase in environmental concerns regarding the emission of

greenhouse gases from conventional power plants, and the desire to generate power locally to improve system efficiency, a significant attention has been prompted toward increasing the injection levels of DG in the system. Moreover, mostly the DG units based on renewable energy resources like PV systems and wind farms have received significant attention. However, the traditional distribution system with uni-directional flow of power from distribution substation to the end users, may not be able to withstand the proliferation of DG.

Different solutions to these issues have been proposed and they usually imply modifying operation settings of existing components such as line voltage regulators and regulating the output of DG units. Although these solutions generally work for low injections of DG, large penetration levels require more complex and expensive approaches. However, all of these solutions are a temporary fix to the problem.

In order to accommodate the increasing penetration levels of Distributed Generation (DG), meshed operation of distribution systems is investigated in this thesis. Given adequate control, protection and automation systems, closed-loop operation of distribution feeders leads to increased reliability and efficiency, reduced voltage drop and losses, and more efficient use of available feeder capacity.

The problem is to compare distribution system meshed configuration with radial configuration with respect to its capability of withstanding higher DG injections. In order to validate the superior behavior of meshed configuration, the maximum allowable DG injection into the distribution system should be calculated and then compared in radial and meshed configurations. In this thesis, this maximum injection has been calculated considering steady state voltage and current limits.

Determining this maximum injection can be done using repetitive power flow methods, as will be explained in chapter 2. Since the number of buses in a distribution system is significantly large, using a method which requires repetition of power flow methods will impose a high computational burden. This is not desired in the distribution system, since the calculation of maximum allowable DG injection depends on the load level. In cases of having a PV system or a wind farm in the system whose output level change dynamically, the maximum allowable DG output for other buses should be calculated dynamically as well. The changes in loads and also generation in the system will lead to the need to calculate maximum allowable DG injection more frequently, requiring a faster approach.

In order to overcome this issue, sensitivity analysis of the active and reactive power injections with system voltages using Jacobian matrix of Newton-Raphson power flow have been considered in this thesis. Therefore, the approach for solving the problem in this thesis is as follows:

- The power flow is run once to determine the system voltages in the base case (without DG).
- A closed form equation is developed to relate changes between injected power from the DG and system voltages. Using this equation, the maximum allowable DG injection considering voltage limits is achieved without requiring power flow iterations.
- Using the previous closed form equation, system voltages are updated in case of having the DG connected to the system and injecting the maximum allowable power based on voltage limits. Then, line currents are checked

for violations of their limits. If any violation has occurred, the previous amount of DG injection is reduced until no violation occurs. In all these steps, there is no need to run power flow.

Alternative meshed operation of distribution systems, viewed as a more long-term systematic solution to increase maximum allowable DG penetration, can then be evaluated using the described metrics. Results for a 69 bus test case are presented for the radial system as well as for select meshed configurations. The obtained results verify the ability of meshed networks to accommodate proliferation of DG.

### 1.7 Organization of Thesis

This thesis is organized as follows:

- In Chapter 2, the method to determine the maximum allowable DG injection based on steady state voltage and current limits is presented. The presented method uses the results of a power flow algorithm, such as Newton-Raphson, in the system without the DG as the base results to investigate the effects of DG injection on system voltages and currents using the sensitivity analysis approach.
- In Chapter 3, the effects of changes in system configuration on the maximum allowable DG injection are studied; specifically, the expected changes of forming a loop in the system are analyzed.
- In Chapter 4, the hypothesis that meshed configuration allows for higher penetration levels of DG is examined using the proposed method in Chapter 3 on a real test system in both single- and multi-DG scenarios.
- Finally, Chapter 5 presents the research accomplishments and contributions of this thesis and presents a discussion of the future work and vision.

## CHAPTER 2: METHODS TO DETERMINE MAXIMUM ALLOWABLE DG INJECTION

### 2.1 Overview

Maximum allowable penetration levels of Distributed Generation (DG) for different configurations of the distribution system are determined in this thesis. The main goal is to compare this maximum value for radial and meshed configurations and verify the hypothesis that meshed configurations may allow higher DG penetration levels. Calculating this maximum value can be done using the repetitive power flow method or it can be estimated via sensitivity analysis.

In this chapter, the repetitive power flow method is presented first. Then, the proposed method for determining maximum allowable DG injection in the distribution system is discussed. Both methods consider the steady-state voltage and current limits. Repetitive power flow method considers a small power injection at the bus whose maximum allowable injection is to be calculated. Then, it checks all voltage and current limits for violations. If no violation has occurred, the injected power is increased until a violation happens, and the final injection would determine the maximum allowable injection at the bus under study. Although accurate, this method requires repetition of power flow for each value of power injection. As explained in the previous chapter, in power distribution systems, it is preferred to avoid running repetitive power flow since it requires significant amount of time and computational burden. On the other hand, the proposed sensitivity analysis approach runs power flow only once in the system without



DG. Then, using closed-form equations based on the Jacobian matrix of Newton-Raphson power flow method, it determines the maximum allowable DG injection which does not violate any voltage or current limits in the system.

## 2.2 Repetitive Power Flow Method

The maximum allowable real power that a DG can inject into the distribution system, based on steady-state voltage and current limits, can be determined using successive power flow solutions. Typically in distribution systems, bus voltages are required to be between 0.95 per unit (p.u.) and 1.05 p.u., and both upper and lower limits are important and need to be considered. Overvoltages will harm the appliances since they have been designed to tolerate the specific voltage limit, and undervoltages will also affect some appliances, such as motors. While this is a general trend and accepted in almost all distribution systems, except otherwise indicated by the operator, line current limits are more dependent on the structure of the system. The current in the lines should not exceed a certain limit. Line current limits are not equal for all branches in a system and are specified by the system operator. This is mainly due to the differences in line types used in different systems or different parts of a system, which changes the conductor temperature they can handle, and hence their loadability limits.

In the repetitive power flow approach, power injection at the specified bus where the DG is to be connected is set to an initial value. Then, using a power flow method, bus voltages in the system are calculated. Using these voltages, current flows in the lines are also determined. All bus voltages and line currents are checked for violations of their allowable limits. The active power injection is then increased by one step, and reactive power injection is also updated knowing the power factor of the DG ( $pf$ ). Then, all the

previous calculations of voltages and currents are repeated to check if any voltage or current has exceeded its allowable limits. This iterative procedure is continued until a single violation in whether bus voltages or line currents has occurred. A flowchart describing the repetitive power flow method is presented in Figure 2.1. It is to be noted that since in the system without DG, all voltages and current are in the desired limit, the iterative procedure is run at least for one iteration of increasing the injected power ( $P_{injected}$ ) at the desired bus.

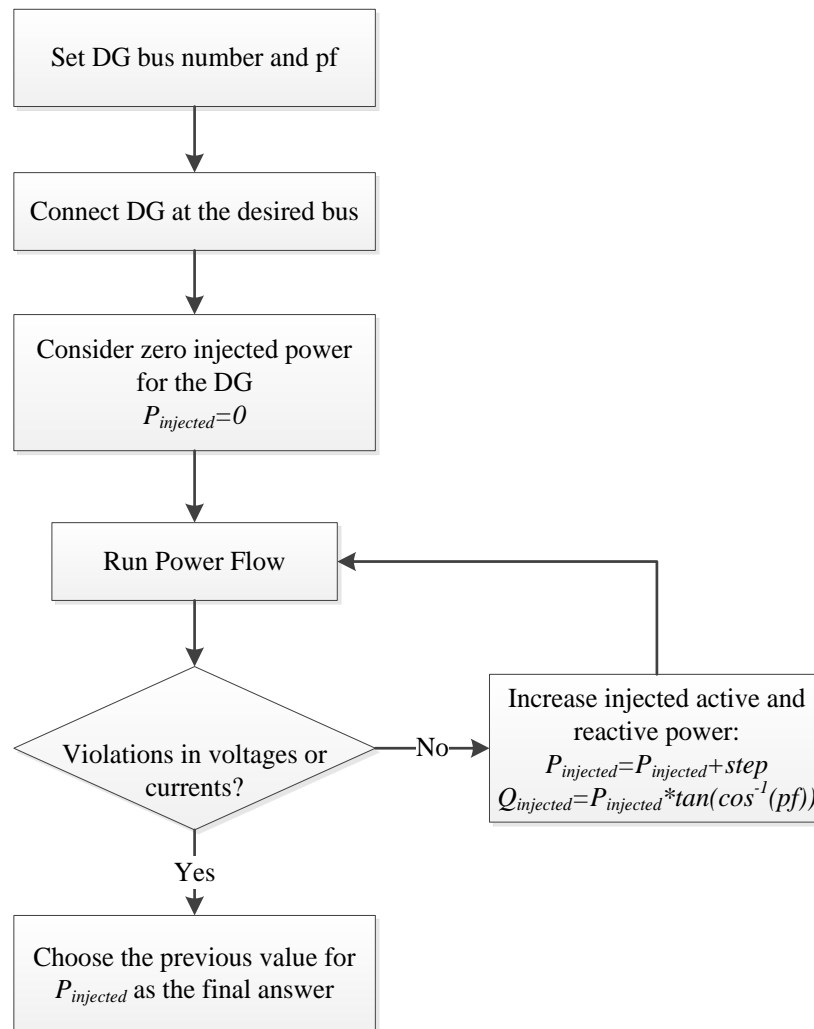


Figure 2.1: Repetitive power flow method for determining maximum allowable power injection at a bus

The repetitive power flow approach requires running power flow in each iteration. Power flow equations, by nature, are nonlinear equations between voltage and power quantities in the system. In more details, if the currents in the system are known, linear equations could be solved for node voltages. However, since powers are usually known in a power system, the equation set becomes the nonlinear set relating powers and voltages. In order to solve this nonlinear set of equations, iterative solution methods are required, such as the Newton-Raphson method. In distribution systems, where number of buses is large, running power flow has a high computational burden. Moreover, running this highly burdened power flow in each iteration until the final answer is achieved takes a lot of time. Thus, it is preferred to avoid the repetitive power flow method for determining maximum allowable injection at a bus. Doing so will enable the operator to update this maximum allowable value dynamically with changes in load, sun irradiance in case of using PV systems as the DG, and other dynamic parameters.

### 2.3 Proposed Method for Determining Maximum Allowable DG Injection Based on Steady State Voltage and Current Limits

In the repetitive power flow method, power flow is performed for each value of DG power injection. However, sensitivity analysis can be used to avoid repetition and to achieve a closed form equation to determine the maximum allowable power injection at a desired bus.

By running power flow on the base case, before connecting the DG at the bus where its maximum allowable DG injection is to be determined, voltages and currents in the system are calculated. In this thesis, these values are referred to as the “base case” values. From the base case results, DG power injection can be related to voltages and

currents in the system, and this relation can be used for calculating maximum allowable DG power injection at each bus. This approach is presented in detail in the next two subsections: in 2.3.1, Considering Bus Voltages, and in 2.3.2, Considering Line Currents. In the first subsection, the proposed method to calculate the maximum allowable injection based on steady-state bus voltages is presented; in 2.3.2, the method is extended to include also line current limitations.

### 2.3.1 Considering Bus Voltages

According to the Newton-Raphson power flow analysis [33] and given the base case power flow results, changes in voltage magnitudes and phases ( $\Delta\delta$  and  $\Delta V$ ) can be related to changes in active and reactive power ( $\Delta P$  and  $\Delta Q$ ) by a linearization around the base case results, using the load flow Jacobian matrix [30][33]:

$$\begin{bmatrix} \Delta P \\ \Delta Q \end{bmatrix} = \begin{bmatrix} J_1 & J_2 \\ J_3 & J_4 \end{bmatrix} \begin{bmatrix} \Delta\delta \\ \Delta V \end{bmatrix} \quad (1)$$

where  $\Delta P$  and  $\Delta Q$  are vectors of changes in bus active and reactive power from the base case, and  $\Delta\delta$  and  $\Delta V$  are vectors of changes in bus voltage angles and magnitudes, respectively. For an  $n$  bus system with  $m$  voltage-controlled buses, the sub-matrices of the Jacobian, namely  $J_1$ ,  $J_2$ ,  $J_3$  and  $J_4$ , will have dimensions  $(n-1) \times (n-1)$ ,  $(n-1) \times (n-1-m)$ ,  $(n-1-m) \times (n-1)$  and  $(n-1-m) \times (n-1-m)$ , respectively [33]. It is to be noted that the substation is not considered in the above equation, since it acts as the system slack bus. Moreover, DG units are not usually participating in voltage control [30]. Therefore, the aforementioned dimensions would be  $(n-1) \times (n-1)$ , and  $J_1$ ,  $J_2$ ,  $J_3$  and  $J_4$  will be invertible.

Assuming there are no changes in the reactive power, i.e.  $\Delta Q = 0$ , the relationship between  $\Delta P$  and  $\Delta V$  is achieved as follows:

$$\Delta P = (J_2 - J_1 J_3^{-1} J_4) \Delta V = J_{RPV} \Delta V \quad (2)$$

where  $(J_{RPV})_{(n-1) \times (n-1)}$  is the matrix which shows the relation between  $\Delta P_{(n-1) \times 1}$  and  $\Delta V_{(n-1) \times 1}$ . Hence, impact of changes in injected active power on the system voltages could be achieved as:

$$\Delta V = V - V^0 = J_{RPV}^{-1} \Delta P \quad (3)$$

where  $(V^0)_{(n-1) \times 1}$  is the base case vector of bus voltage magnitudes, excluding the slack bus, and  $V_{(n-1) \times 1}$  is the vector of new bus voltage magnitudes. Following the same procedure, the relation between changes in the injected reactive powers and changes in the system voltages would be:

$$\Delta Q = (J_4 - J_3 J_1^{-1} J_2) \Delta V = J_{RQV} \Delta V \quad (4)$$

where  $(J_{RQV})_{(n-1) \times (n-1)}$  is short form of the term in parentheses, which shows the relation between  $\Delta Q_{(n-1) \times 1}$  and  $\Delta V_{(n-1) \times 1}$ . Changes in the system voltage magnitudes due to changes in injected reactive powers would then be:

$$\Delta V = V - V^0 = J_{RQV}^{-1} \Delta Q \quad (5)$$

Therefore, considering changes in active and reactive powers based on the superposition theorem, the total changes in system voltages would equal the summation of the changes due to  $\Delta P$  and  $\Delta Q$ :

$$\Delta V = V - V^0 = J_{RPV}^{-1} \Delta P + J_{RQV}^{-1} \Delta Q \quad (6)$$

In order to evaluate the effect of injected active power by a DG connected at bus  $j$ ,  $P_j$ , on the voltage of bus  $i$ ,  $V_i$ , (6) can be written as:

$$\Delta V_i = V_i - V_i^0 = J_{VPQ_{ij}} P_j \quad (7)$$

where  $J_{VPQ_{ij}}$  is the  $(i,j)$  element of the matrix  $J_{VPQ}$  which is calculated by the following equation:

$$J_{VPQ_{ij}} = J_{RPV_{ij}}^{-1} + J_{RQV_{ij}}^{-1} \tan(\cos^{-1}(pf_j)) \quad (8)$$

where  $pf_j$  is the power factor angle of the DG at bus  $j$ . Hence, the value of injected active power that leads to a  $\Delta V$  change in the voltage magnitude of bus  $i$  is determined as:

$$P_j = \frac{\Delta V_i}{J_{VPQ_{ij}}} \quad (9)$$

Based on the sign of  $J_{VPQ_{ij}}$ , increasing  $P_j$  will lead to either an increase (for positive values of  $J_{VPQ_{ij}}$ ) or a decrease (for negative values of  $J_{VPQ_{ij}}$ ) in the bus  $i$  voltage. Therefore, if  $J_{VPQ_{ij}}$  is positive, knowing the base case results for the voltage magnitude at bus  $i$  ( $V_i^0$ ), the maximum allowable variation of  $V_i$  from this value (i.e. before the upper threshold for the voltages is exceeded) can be calculated as (10):

$$\Delta V_i^{Max} = V^{upper\_threshold} - V_i^0 \quad (10)$$

On the other hand, if  $J_{VPQ_{ij}}$  is negative, the maximum allowable variation of  $V_i$  from the base case voltage magnitude would be:

$$\Delta V_i^{Max} = V^{lower\_threshold} - V_i^0 \quad (11)$$

The maximum allowable variation in bus  $i$  voltage should be considered for determining the maximum allowable power injection at bus  $j$  due to the voltage limits on bus  $i$ . The maximum allowable active power injection at bus  $j$  based on the voltage limits at bus  $i$  is:

$$P_j^{Max,i} = \frac{\Delta V_i^{Max}}{J_{VPQ_{ij}}} \quad (12)$$

The amount of power injection at bus  $j$  should not cause the voltage in any bus in the system to violate the desired limits. Hence, based on the voltage limit criteria, the maximum allowable generation at bus  $j$  in a system of  $n$  buses can be determined as:

$$P_j^{Max,V} = \underset{i=2,n}{Min}\{P_j^{Max,i}\} \quad (13)$$

Since the capacities of DG units are also limited, the maximum allowable injected power should not exceed this limit. Moreover, in some cases, the total amount of DG power injection is limited based on the total load of the system. For instance, a DG might not be allowed to inject an amount of power that causes the flow of power from the distribution system toward the substation, whereas in some cases, this might be of interest. In general, the maximum allowable power injection at a certain bus considering the bus voltage criteria as well as the DG capacity is denoted by  $P_j^{Max,V,DG}$  in this thesis. This value is the minimum of  $P_j^{Max,V}$ , calculated by (13), and the value of DG capacity and the DG power output limit considering the total load of the system:

$$P_j^{Max,V,DG} = \underset{}{Min}\{P_j^{Max,V}, P_j^{Max,DG\_Capacity}, P_j^{Max,Grid\_requirements}\} \quad (14)$$

The procedure of finding  $P_j^{Max,V,DG}$  is depicted in the flowchart of Figure 2.2.

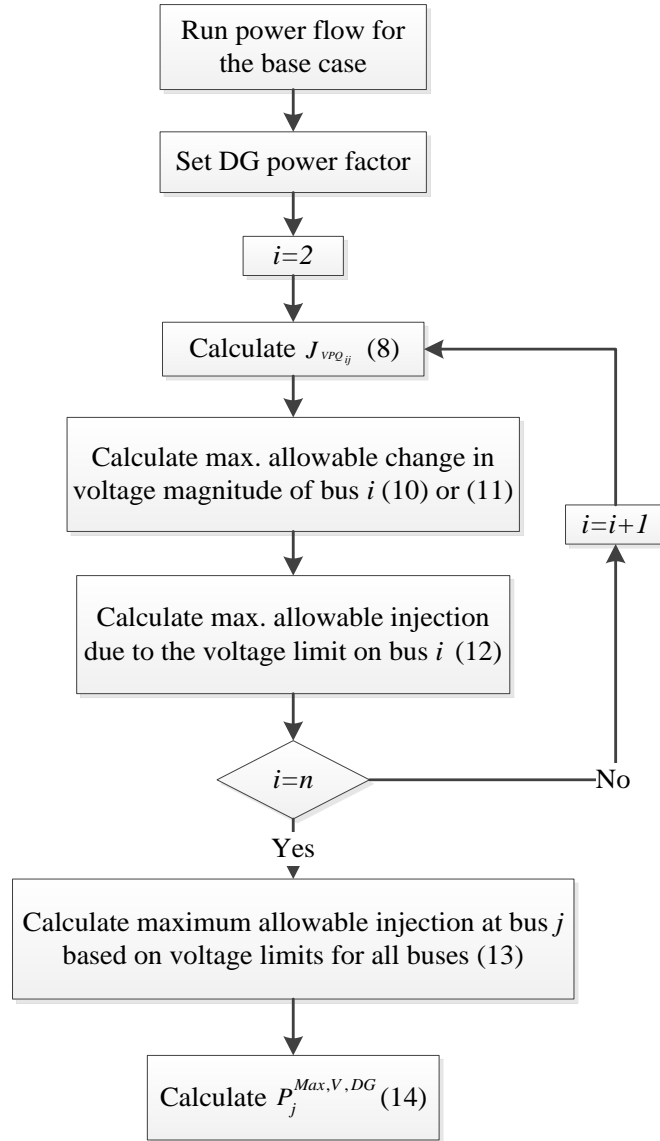


Figure 2.2: Flowchart for determining maximum allowable DG injection based on voltage limits and DG capacity

### 2.3.2 Considering Line Currents

The maximum allowable output power of a DG should also meet another important set of criteria: it should not cause distribution lines to be loaded beyond their current carrying capacities. Once the maximum allowable DG output power at a specific bus in the system is determined as  $P_j^{Max,V,DG}$ , the currents in the system where a DG with



injection equal to  $P_j^{Max,V,DG}$  is connected at bus  $j$  are checked to see if they exceed their operating limits. If the currents are violating the desired limits, the amount of maximum allowable DG penetration is decreased until no single violation occurs in the system.

Power flow methods can be used to calculate the currents in case of having a DG in the system. Since the aforementioned procedure requires repetition until no current violation is seen in the system, using power flow methods will require significant amount of time and will put a high computational burden. Instead of using the repetitive power flow methods, one can use closed form equations to update voltages in case of having the DG connected to the system, using the base case results (as shown in 2.3.1). Then, the currents could be updated using the updated voltage values, and these updated currents are checked to satisfy the desired limits. The general procedure will still require repetitions for each value of DG power output; however, using closed form equations will reduce the computational burden and time for each iteration in comparison with the repetitive power flow methods.

Figure 2.3 shows the procedural flowchart to determine maximum allowable injection of a DG connected at bus  $j$ , where steady-state current limits are also considered. Initially, the value of injected power from the DG at bus  $j$ ,  $P_{injected}$ , is set as  $P_j^{Max,V,DG}$ . Voltage magnitudes and angles are updated by using the base case power flow results and without re-running the power flow for the updated system with the DG. As an expansion of (7), voltage magnitudes at bus  $i$  due to the power injection at bus  $j$  is calculated by:

$$V_i = V_i^0 + J_{VPQ_{ij}} P_{injected} \quad (15)$$

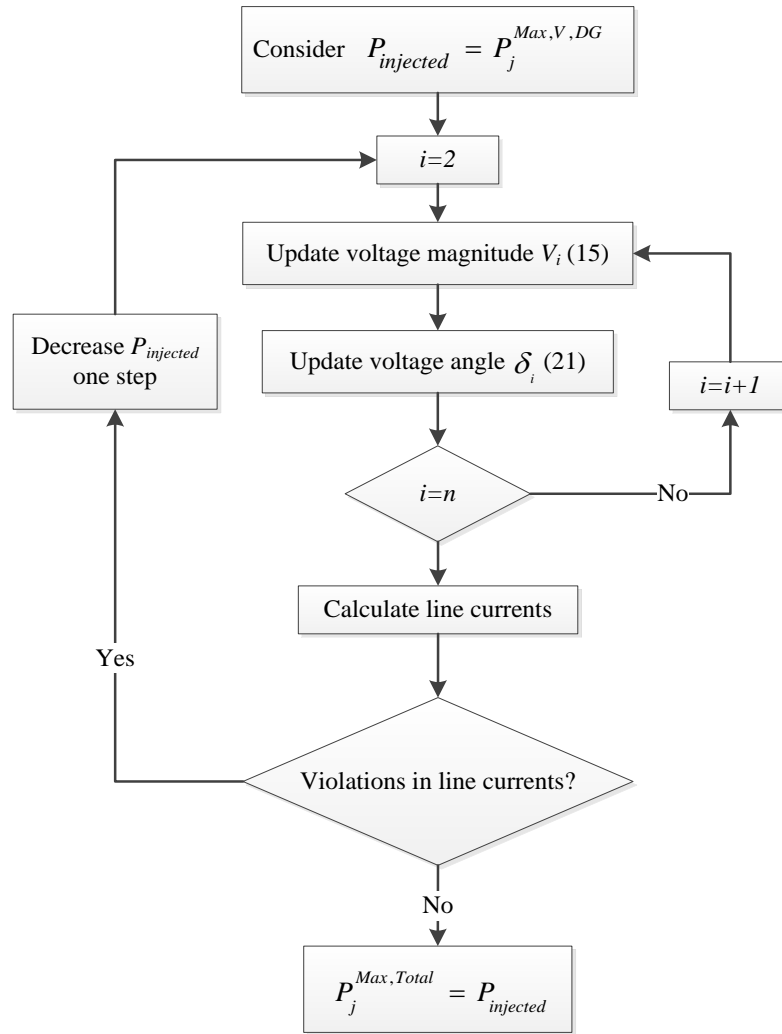


Figure 2.3: Determining the maximum allowable generation of a DG

Using (15), voltage magnitudes at all buses (except for the slack bus) are updated. A similar approach to what was used to derive (8) can be used for updating voltage angles. Using (1), the relationships between  $\Delta P$  and  $\Delta \delta$  when  $\Delta Q$  is assumed to be zero, and between  $\Delta Q$  and  $\Delta \delta$  when  $\Delta P$  is assumed to be zero, are as described in (16) and (17), respectively:

$$\Delta P = (J_1 - J_2 J_4^{-1} J_3) \Delta \delta = J_{RPD} \Delta \delta \quad (16)$$

$$\Delta Q = (J_3 - J_4 J_2^{-1} J_1) \Delta \delta = J_{RQD} \Delta \delta \quad (17)$$

where  $\Delta \delta_{(n-1) \times 1}$  is the vector of changes in voltage angles, and  $J_{RPD}$  and  $J_{RQD}$  are the matrices relating  $\Delta P$  and  $\Delta Q$  to these changes, respectively. The changes in voltage angles as effects of both active and reactive power variations are calculated as:

$$\Delta \delta = \delta - \delta^0 = J_{RPD}^{-1} \Delta P + J_{RQD}^{-1} \Delta Q \quad (18)$$

where  $\delta_{(n-1) \times 1}^0$  is the vector of base case voltage angles. Knowing the DG active power and power factor at bus  $j$ , the change in bus  $i$  voltage angle is calculated as:

$$\Delta \delta_i = \delta_i - \delta_i^0 = J_{DPQ_{ij}} P_j \quad (19)$$

where:

$$J_{DPQ_{ij}} = J_{RPD_{ij}}^{-1} + J_{RQD_{ij}}^{-1} \tan(\cos^{-1}(pf_j)) \quad (20)$$

Therefore, similar to (14), the voltage angle at bus  $i$  due to the DG power injection at bus  $j$  is calculated as:

$$\delta_i = \delta_i^0 + J_{PDQ_{ij}} P_{injected} \quad (21)$$

Using (21), voltage angles at all system buses (except the slack bus) are also updated. Knowing the voltage magnitudes and angles, line currents can be calculated. All calculated line currents are then checked to see if they exceed their operating limits. If a single line has exceeded its current criterion, the amount of maximum allowable power injection at bus  $j$  needs to be decreased. This can be done iteratively until no current violation is observed in the system. In this paper, the initial decrements are set to 1% of

the previous value of injected power. The final result will be  $P_j^{Max,Total}$ , which considers all the required criteria.

It is important to note that the power flow results are calculated only once for the base case system - with no DG connected at bus  $j$  - and then the value of maximum allowable  $P_j^{Max,Total}$  is determined using the proposed approach. It is noted that the base case might include one or more DG units at other buses, and their power injection is considered in the power flow algorithm. Therefore, base case results, achieved only once from power flow, denote system voltages and currents while there is no DG connected to the bus at which its maximum allowable generation is to be calculated. Therefore, using the proposed approach, multi-DG scenarios can also be analyzed.

In the next chapter, possible effects of distribution system configuration on the maximum allowable DG output are analytically studied. Then, in chapter 5, the proposed method has been applied to a 69 bus test system to compare maximum allowable DG penetration under different distribution system configurations. Multi-DG scenarios have also been considered as test cases.

## CHAPTER 3: EFFECTS OF CHANGING DISTRIBUTION SYSTEM CONFIGURATION

### 3.1 Overview

Distribution system configuration denotes the topological structure in which elements of the system are connected together to form an interconnected system, which includes buses, lines, transformers, normally-closed (sectionalizing) switches, normally-open (tie) switches, and so on. Keeping the same number and position of buses in the system, changing the configuration of the distribution system will change the connections between system buses. Even if the power injections from these buses remain constant, this change in system configuration will in turn affect voltage profile in the system and also change the currents in the lines. The goal of this chapter is to analyze the effects of changing the system configuration and its resulting effects on the maximum allowable DG power injection in the system.

### 3.2 Expected Changes in DG Maximum Allowable Power Injection

DG power injection at a specific bus affects system voltages and line currents, and is allowed to increase before any violation in these quantities occurs. In the previous chapter, a method was proposed to determine this maximum allowable power injection from a DG based on steady-state voltage and current limits. In this subsection, the effects of changing the system configuration on the factors which play a role in determining the system voltages and currents, and hence the maximum allowable DG power injection, are analyzed. Specifically, adding a tie line between two existing buses forming a loop in the

distribution system is investigated.

Based on the concept of node-voltage equations [33], the governing equation between node voltages and injected currents from the nodes to the system is achieved as:

$$I_{bus} = Y_{bus} \times V_{bus} \quad (22)$$

where  $I_{bus}$  is the vector of injected bus currents,  $V_{bus}$  is the vector of bus voltages (measured from the reference node, i.e. ground), and  $Y_{bus}$  is the bus admittance matrix.

$I_{bus}$  will have positive values in buses that inject current towards the system, which are actually the buses with generation. In other buses, where loads absorb power, the current is drawn from the system, and  $I_{bus}$  has negative values. The diagonal elements of the  $Y_{bus}$  corresponding to each node, node self-admittances, are the summation of all admittances connected to that node. Therefore, considering node  $p$ , its self-admittance is:

$$Y_{pp} = \sum_{q=0}^n y_{pq} \quad q \neq p \quad (23)$$

where  $q$  shows all other nodes (except node  $p$ ), and  $y_{pq}$  is the admittance of the line between nodes  $p$  and  $q$ . It is to be noted that  $q$  can be zero, referring to the ground, and  $y_{pq}$  denotes the load connected to bus  $p$ . Off-diagonal element is the negative value of the admittance between each two corresponding buses, calculated as:

$$Y_{pq} = -y_{pq} \quad (24)$$

Knowing  $I_{bus}$ , bus voltages can be found from:

$$V_{bus} = Y_{bus}^{-1} \times I_{bus} \quad (25)$$

where the inverse of  $Y_{bus}$  is the bus impedance matrix,  $Z_{bus}$ .

Consider line  $l$  is added between two existing buses, bus  $m$  and  $n$ . The injected active and reactive powers in the system remain constant, and for simplicity, it is assumed that their current injections are also kept constant. Moreover, it is assumed that the current absorbed by load buses remains constant, regardless of their load type. Using (23) and (24), the new  $Y_{bus}$  can be determined. It is clear that the only values changed in this matrix are  $Y_{mm}$ ,  $Y_{nn}$ ,  $Y_{mn}$ , and  $Y_{nm}$ . However, all elements of  $Z_{bus}$  matrix will change. Since the voltages are to be calculated from injected currents using (25), bus voltages are changed due to the addition of a line between two buses. The change in bus voltages can also be viewed as a reason of the change in current flows in other lines when a line is added to the system.

A bus voltage may be increased or decreased due to forming a loop in the system. This depends on the topology of the system, location of the loads around the bus, location of the new line in regards to the bus, and changes in the current flows in the lines. All these factors might either boost the voltage up, or decrease it. As discussed earlier, studies have shown that the voltage profile of the system is improved in case of having meshes in the system, i.e. the bus voltages are increased [3][8][26]. Although it depends on the specific system under study, forming a loop at the end of the feeder will typically increase the voltage at buses located at the end of the feeder. After forming the loop, the end-lateral bus will in fact be closer to the substation, and the flow of power toward this bus will see less voltage decrease. Some voltages in the system might decrease and the details will be explained with examples in the next chapter. However, the general conclusion can be made that changing the voltage magnitudes in the base case- without connecting the DG at the bus where its maximum allowable injection is to be determined-

changes the maximum allowable power injection based on voltage and current limits. Therefore, any change in the system configuration that changes the base case voltages and current will change the maximum allowable injection in the system. This is discussed in the next paragraphs.

If the maximum allowable DG injection at bus  $j$  considering the steady state voltage limits is to be calculated, all bus voltages need to be considered, as described in (13):

$$P_j^{Max,V} = \text{Min}\{P_j^{Max,i}\}_{i=2:n} \quad (13)$$

For a bus  $i$ , consider its voltage before and after forming the loop as  $V_i^{radial}$  and  $V_i^{meshed}$ , respectively. If  $V_i^{meshed}$  is greater than  $V_i^{radial}$ , and if the power factor and location of the DG at bus  $j$  is such that its generation increases the voltage magnitude at bus  $i$ , then  $\Delta V_i^{Max,meshed}$  will have lower value than  $\Delta V_i^{Max,radial}$ . If the effect of changes in system configuration is not considered in (12):

$$P_j^{Max,i} = \frac{\Delta V_i^{Max}}{J_{VPQ_{ij}}} \quad (12)$$

the value of  $P_j^{Max,i,meshed}$  is less than  $P_j^{Max,i,radial}$ .

If the previous assumption is true, then based on the general idea that meshing the system boosts the voltages, it might be concluded that meshing will decrease the amount of maximum generation allowed in the system. However, besides changes in system voltages, since  $Y_{bus}$  changes as a result of system configuration changes, the Jacobian matrix used in (1) will also change.  $J_1$ , which shows the sensitivity of changes in voltage



angles to changes in active power injection, has the diagonal and off diagonal elements shown in (26) and (27), respectively.

$$J_{1_{ii}} = \sum_{j \neq i} |V_i| |V_j| |Y_{ij}| \sin(\theta_{ij} - \delta_i + \delta_j) \quad (26)$$

$$J_{1_{ij}} = -|V_i| |V_j| |Y_{ij}| \sin(\theta_{ij} - \delta_i + \delta_j) \quad , j \neq i \quad (27)$$

where  $\delta_i$ ,  $\delta_j$ , and  $\theta_{ij}$  are angles of  $V_i$ ,  $V_j$ , and  $Y_{ij}$ , respectively. As seen in above equations,  $J_1$  values will change, both due to the changes in voltages and  $Y$  bus matrix elements. Other sub-matrices of Jacobian matrix will change in a similar manner. Then, according to (2) and (4),  $J_{RPV}$  and  $J_{RQV}$  will also change. This, in turn, will change the values of  $J_{VPQ}$ .

Therefore, the two main factors in (12) for calculating the maximum allowable generation at bus  $j$  only based on steady state voltage limit on bus  $i$ , namely  $\Delta V_i^{Max}$  and  $J_{VPQ_j}$ , will change due to adding a new line in the system. The maximum allowable changes in the voltage of bus  $i$  will change, since the system configuration affects system voltages. The value of  $J_{VPQ_j}$  will also change, both due to the change in system voltages and the change in  $Y_{bus}$ . Based on (13), all bus voltages should be considered for determining  $P_j^{Max,V}$ . Therefore, changes in  $P_j^{Max,i,meshed}$  for all  $i$  values should be considered to compare the maximum allowable generation at bus  $j$  based on steady state voltage limits of all buses in both system configurations.

The other important set of criteria for determining  $P_j^{Max,Total}$  are line currents limits. Assuming that meshing the system allows more generation at bus  $j$  based on

voltage limits, a change in the configuration also changes the pattern for current flows in the lines. Adding a new line in the system will create new paths for the currents to flow, and reduces line exploitation [3][8][26]. Therefore, it can be assumed that the DG at bus  $j$  is allowed to inject more power in the meshed case before a current in the system is violated.

In general, changes in system configuration will change the maximum allowable generation in system buses. This change might be an increase for some buses, and decrease for others. The assumptions and considerations made in this chapter will be analyzed in the next chapter and the results achieved for a test case system will be presented.

## CHAPTER 4: ASSESSMENT OF DISTRIBUTION SYSTEM MESHED CONFIGURATION FOR INCREASED DG PENETRATION: A CASE STUDY

### 4.1 Overview

For validation and demonstration purposes, the proposed method for determining the maximum allowable DG generation in the system has been applied to a test system, and results are compared between radial and meshed system configurations. A 69 bus real system with two different demand scenarios has been used as test system. The results have been presented for different power factors and locations of DG units in radial and meshed configurations. Then, cases containing multiple DG units in the system have been analyzed. The main goal is to compare the maximum generation that a DG/ a system of DG units are allowed to inject to the system in different system configurations, and verify the theory presented in the previous chapter that select meshed configuration may allow for higher penetration of DG units in the system.

In the next section, the test case distribution system is presented. In Section 4.3, the effects of system configurations on maximum allowable DG power injection are studied. In Section 4.4, the effects of DG power factor on this maximum value are analyzed for different system configurations. Section 4.5 presents the results for cases with multiple DG units in the system and compares the performance of meshed and radial configurations with respect to their allowable DG penetration levels. Section 4.6 presents a summary of results and observations.

## 4.2 System Specification: 69 Bus Test System

The single line diagram of the 69 bus test system used in this thesis is shown in Figure 4.1 [30][34][35]. The system nominal voltage is 12.66 kV, and base power for the calculations is considered equal to 10 kVA. The system presents both residential and commercial loads. Two different load demand scenarios are considered. The maximum demand scenario is characterized by the total active and reactive power demands of 3802.2 kW and 2694.6 kVAr, respectively, as shown in Table 4.1. The minimum demand scenario has total load equivalent to 20% of the maximum demand scenario.

Voltage at the substation is set to 1.04 per unit (pu) in both demand scenarios in order to keep all bus voltage magnitudes in the desired range of 0.95 pu and 1.05 pu. Line current limit is 400 A for branches 1-9, 300 A for branches 46-49 and 52-64, and 200 A for all other branches including tie lines. The system has 73 branches, including 5 tie lines, which are normally open and can each be closed with a tie switch for forming different meshed structures. The data related to the lines is presented in Table 4.2 [35]. For simplicity, the meshed configuration obtained by closing  $T_i$  is named  $C_i$ .

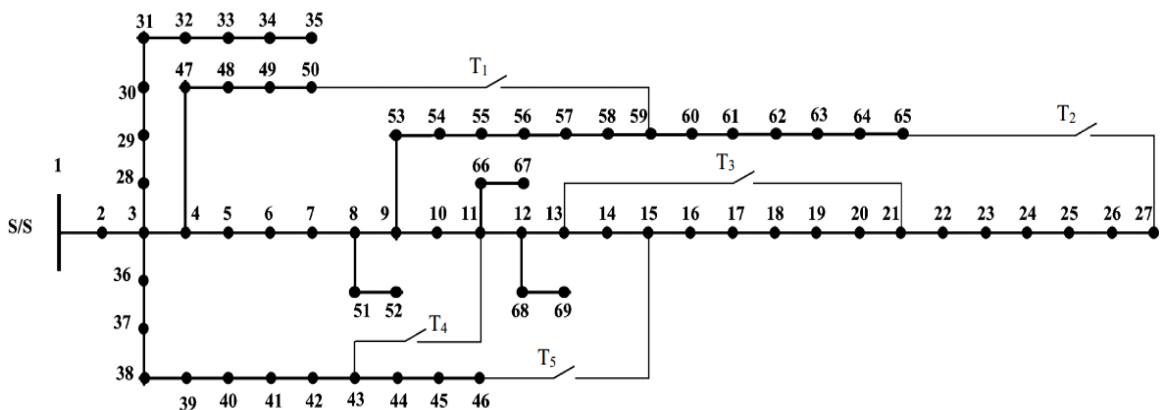


Figure 4.1: Test case system [5]

Since the maximum total load of the system is 3.802 MW and the distribution system does not require a DG with an output higher than this value, the DG capacities are indicatively limited to 4 MW.

In the following sub-sections, maximum allowable DG penetration in the system is determined for different system configurations and DG power factors. Results show the ability of meshed configurations to allow for higher penetration levels in the system.

Table 4.1: Load data for the maximum demand scenario

Bus	P <sub>load</sub> (kW)	Q <sub>load</sub> (kVAr)	Bus	P <sub>load</sub> (kW)	Q <sub>load</sub> (kVAr)	Bus	P <sub>load</sub> (kW)	Q <sub>load</sub> (kVAr)
1	0	0	24	28	20	47	0	0
2	0	0	25	0	0	48	79	56.4
3	0	0	26	14	10	49	384.7	274.5
4	0	0	27	14	10	50	384.7	274.5
5	0	0	28	26	18.6	51	40.5	28.3
6	2.6	2.2	29	26	18.6	52	3.6	2.7
7	40.4	30	30	0	0	53	4.35	3.5
8	75	54	31	0	0	54	26.4	19
9	30	22	32	0	0	55	24	17.2
10	28	19	33	14	10	56	0	0
11	145	104	34	19.5	14	57	0	0
12	145	104	35	6	4	58	0	0
13	8	5	36	26	18.55	59	100	72
14	8	5.5	37	26	18.55	60	0	0
15	0	0	38	0	0	61	1244	888
16	45.5	30	39	24	17	62	32	23
17	60	35	40	24	17	63	0	0
18	60	35	41	1.2	1	64	227	162
19	0	0	42	0	0	65	59	42
20	1	0.6	43	6	4.3	66	18	13
21	114	81	44	0	0	67	18	13
22	5	3.5	45	39.22	26.3	68	28	20
23	0	0	46	39.22	26.3	69	28	20

Table 4.2: Line data for the test case

Line No.	From Bus	To Bus	R ( $\Omega$ )	X ( $\Omega$ )	Line No.	From Bus	To Bus	R ( $\Omega$ )	X ( $\Omega$ )
1	1	2	0.0005	0.0012	20	20	21	0.3416	0.1129
2	2	3	0.0005	0.0012	21	21	22	0.014	0.0046
3	3	4	0.0015	0.0036	22	22	23	0.1591	0.0526
4	4	5	0.0251	0.0294	23	23	24	0.3463	0.1145
5	5	6	0.366	0.1864	24	24	25	0.7488	0.2475
6	6	7	0.3811	0.1941	25	25	26	0.3089	0.1021
7	7	8	0.0922	0.047	26	26	27	0.1732	0.0572
8	8	9	0.0493	0.0251	27	3	28	0.0044	0.0108
9	9	10	0.819	0.2707	28	28	29	0.064	0.1565
10	10	11	0.1872	0.0619	29	29	30	0.3978	0.1315
11	11	12	0.7114	0.2351	30	30	31	0.0702	0.0232
12	12	13	1.03	0.34	31	31	32	0.351	0.116
13	13	14	1.044	0.345	32	32	33	0.839	0.2816
14	14	15	1.058	0.3496	33	33	34	1.708	0.5646
15	15	16	0.1966	0.065	34	34	35	1.474	0.4873
16	16	17	0.3744	0.1238	35	3	36	0.0044	0.0108
17	17	18	0.0047	0.0016	36	36	37	0.064	0.1565
18	18	19	0.3276	0.1083	37	37	38	0.1053	0.123
19	19	20	0.2106	0.0696	38	38	39	0.0304	0.0355

Table 4.2: (continued)

Line No.	From Bus	To Bus	R ( $\Omega$ )	X ( $\Omega$ )	Line No.	From Bus	To Bus	R ( $\Omega$ )	X ( $\Omega$ )
39	39	40	0.0018	0.0021	57	57	58	0.7837	0.263
40	40	41	0.7283	0.8509	58	58	59	0.3042	0.1006
41	41	42	0.31	0.3623	59	59	60	0.3861	0.1172
42	42	43	0.041	0.0478	60	60	61	0.5075	0.2585
43	43	44	0.0092	0.0116	61	61	62	0.0974	0.0496
44	44	45	0.1089	0.1373	62	62	63	0.145	0.0738
45	45	46	0.0009	0.0012	63	63	64	0.7105	0.3619
46	4	47	0.0034	0.0084	64	64	65	1.041	0.5302
47	47	48	0.0851	0.2083	65	11	66	0.2012	0.0611
48	48	49	0.2898	0.7091	66	66	67	0.0047	0.0014
49	49	50	0.0822	0.2011	67	12	68	0.7394	0.2444
50	8	51	0.0928	0.0473	68	68	69	0.0047	0.0016
51	51	52	0.3319	0.1114	69	50	59	2	1
52	9	53	0.174	0.0886	70	27	65	1	0.5
53	53	54	0.203	0.1034	71	13	21	0.5	0.5
54	54	55	0.2842	0.1447	72	43	11	2	0.5
55	55	56	0.2813	0.1433	73	46	15	1	0.5
56	56	57	1.59	0.5337					



### 4.3 Effect of System Configuration: Radial vs. Meshed

In this section, using the explanation provided in Chapter 4, expectation of meshed configuration for allowing more injected power is examined. Then,  $P_j^{Max,V,Total}$  for all system buses (except for the slack bus) is compared in radial and meshed configurations. For the sake of simplicity, unity power factor is considered for the DG that is going to be connected to the system, and only maximum demand scenario is considered for the system.

#### 4.3.1 Expected Changes Due to Different Configuration: An Example

Consider the test system as shown in Figure 4.1, in which closing tie switch  $T_i$  will form the meshed configuration  $C_i$ . As discussed in chapter 4, adding a new line between two existing buses will change the system  $Y_{bus}$  and hence the  $Z_{bus}$ . Therefore, system voltages will change due to the change in system configuration. Moreover, voltage of a bus might be increased or decreased moving from radial toward meshed structure.

Performing the Newton Raphson power flow for radial and meshed configuration of the test case system, voltages in the system for each configuration are achieved. Figure 4.2 shows bus voltages, for each meshed configuration in comparison with the radial configuration.

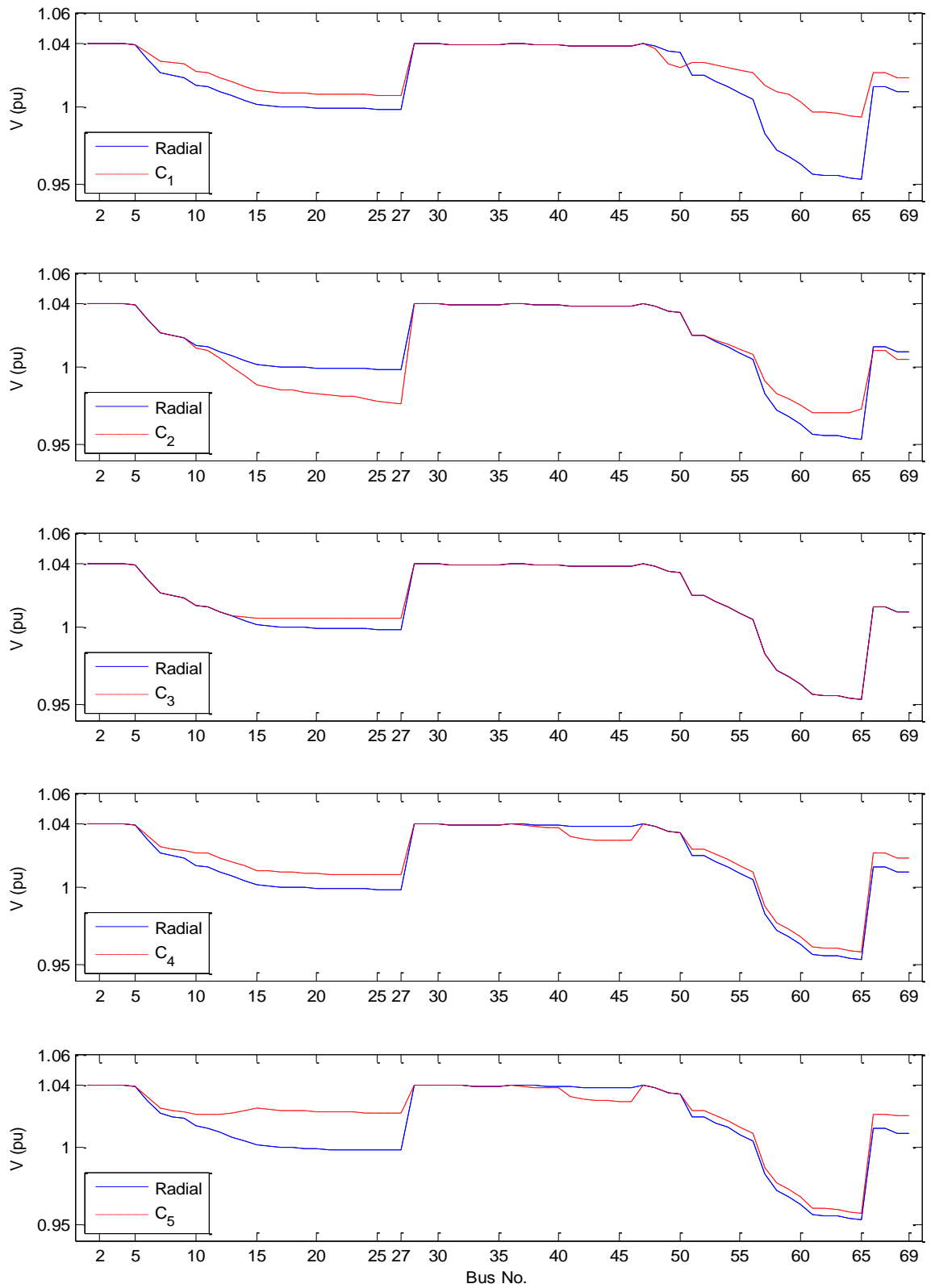


Figure 4.2: Bus voltages in different system configurations in maximum demand scenario without DG

As can be seen in Figure 4.2, changing system configuration has different effects on system voltages. For example, meshed configuration  $C_1$  increases the voltages at bus 20, while decreases the voltage at bus 50. Moreover, changes in bus voltages are directly dependent on the specific meshed configuration. For instance, voltage at bus 27 is increased in meshed configuration  $C_1$  and decreased in meshed configuration  $C_2$ .

Since adding a new line between two existing nodes in the system affects the system  $Y_{bus}$  matrix, according to (23) and (24), the sub-matrices of the Jacobian matrix will also change. Hence, based on (2), (4) and (6), values of  $J_{RPV}$ ,  $J_{RQV}$ , and  $J_{VPQ}$  matrix will be different than in the radial case. In order to calculate the maximum allowable active power injection based on voltage constraints, voltage constraints at all buses need to be considered. In the following paragraphs, the maximum allowable injection at bus 27 in unity power factor due to the voltage limits at the same bus ( $P_j^{Max,i}$ ) is compared under different system configurations to discuss the concepts explained in chapter 3.

For each configuration, voltage of bus 27 in the base case (without DG) is known from power flow solutions. Knowing the maximum and minimum allowable voltage limits, the maximum change in voltage of bus 27 from the base case due to the upper ( $\Delta V_{27}^{Max\_U, Radial}$ ) or lower ( $\Delta V_{27}^{Max\_L, Radial}$ ) voltage limit is calculated. Then, the value of  $J_{VPQ_{27,27}}$  is calculated using (8), considering the appropriate value of allowable changes in voltage of bus 27. Using (12), the maximum allowable generation at bus 27 considering bus 27 steady state voltage limits is determined:

$$P_j^{Max,i} = \frac{\Delta V_i^{Max}}{J_{VPQ_{ij}}} \quad (12)$$

The results for all 6 configurations are provided in Table 4.3.

Table 4.3: Calculating  $P_{27}^{Max,27}$  for different configurations

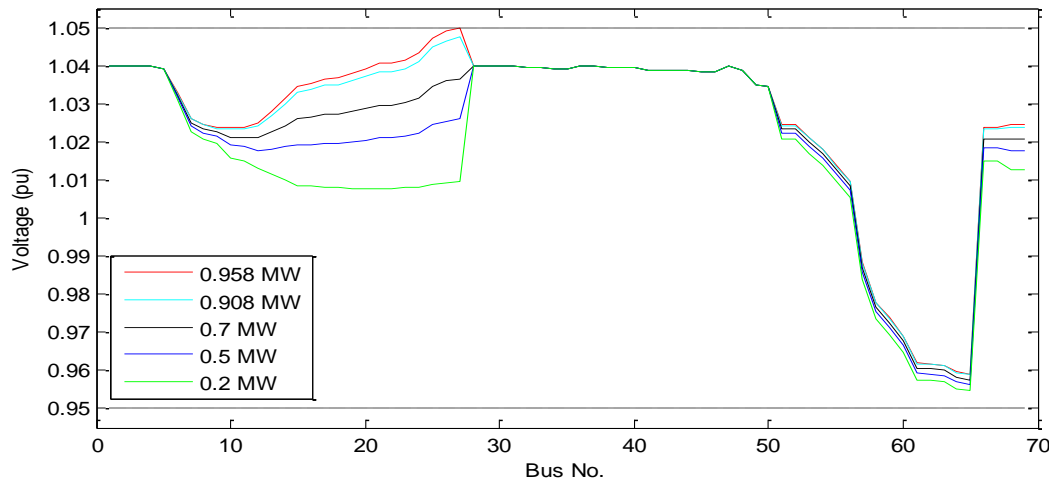
Config.	$V_{27}$ (p. u.)	$\Delta V_{27}^{Max\_U}$ (p. u.)	$\Delta V_{27}^{Max\_L}$ (p. u.)	$J_{VPQ_{27,27}}$	$P_{27}^{Max,27}$ (12)	
					p. u. (10)	MW
Radial	0.9982	0.0518	-0.0482	0.000570	90.8	0.908
$C_1$	1.0071	0.0429	-0.0571	0.000557	77.1	0.771
$C_2$	0.9761	0.0739	-0.0261	0.000321	230.4	2.304
$C_3$	1.0050	0.0450	-0.0550	0.000369	121.7	1.217
$C_4$	1.0073	0.0427	-0.0573	0.000519	82.2	0.822
$C_5$	1.0222	0.0278	-0.0722	0.000307	90.7	0.907

As Table 4.3 reveals, all values of  $J_{VPQ_{27,27}}$  are positive. This means that increasing power injection at bus 27 will increase the voltage at this bus. Hence, the values of  $\Delta V_{27}^{Max\_U}$  are considered for calculating  $P_{27}^{Max,27}$ . Moving from the radial structure to  $C_2$  decreases the voltage of bus 27 in the base case, hence allowing it to increase more before it violates the upper voltage threshold. Moreover, the value of  $J_{VPQ_{27,27}}$  also decreases. These two changes will lead to an increase in the value of  $P_{27}^{Max,27}$ , which is the maximum allowable power injection at bus 27 due to its own voltage limits. Interestingly, the base case voltage of bus 27 for configuration  $C_3$  is higher than the radial case.

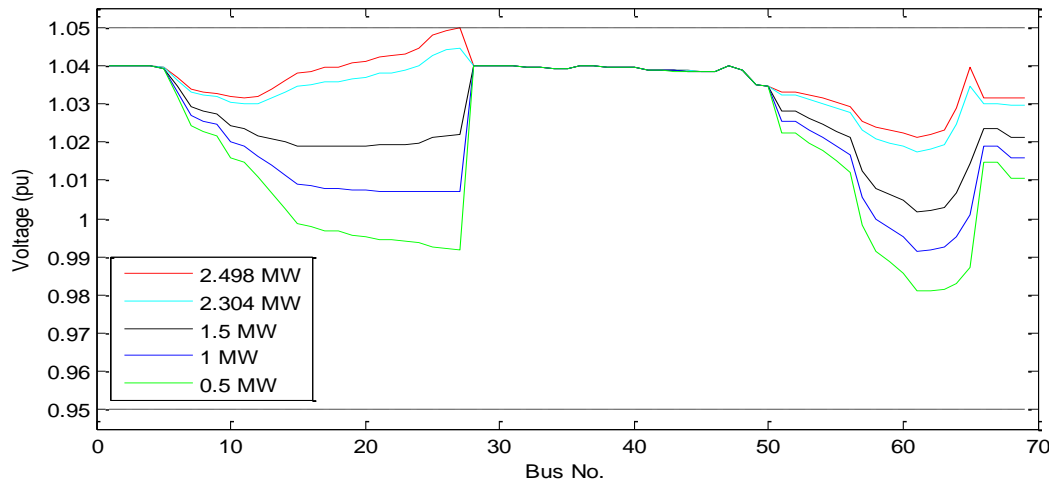
However, changes in the system  $Y_{bus}$  have led to lower value for  $J_{VPQ_{27,27}}$  in the meshed configuration  $C_3$  such that the value of  $P_{27}^{Max,27}$  is increased in this configuration. This analysis shows the effect of changing the system configuration on the maximum allowable injection at bus 27 only due to its own voltage while the final value for maximum allowable injection should consider voltage limits at all buses. Although in the simulations, all bus voltages have been considered for determining  $P_{27}^{Max,V}$ , for the sake of conciseness, these results are not provided. As expected, the simulation results have shown that for bus 27, the first bus that violates the voltage limits, and hence the bus that determines the total maximum allowable injection at bus 27, is bus 27 itself.

As seen in Table 4.3, the maximum power output of a DG working in unity power factor connected to bus 27 without violating voltage limits is 0.908 MW. If the repetitive power flow method was used, this value was obtained as 0.958 MW, which shows good accuracy of the proposed method with a 5.2% absolute error. All conducted studies have shown that the proposed method is conservative for calculating the maximum allowable penetration value in comparison with the repetitive power flow method.

Figure 4.3a shows the voltages of the radially-operated system with DG connected to bus 27 for different values of output power with unity power factor. As can be seen in this figure, the voltages are gradually increased while the output of this DG is increased, and when the output power reaches the calculated value of  $P_{27}^{Max,V}$ , voltage limits are violated. This figure also verifies the result obtained by the proposed method for  $P_{27}^{Max,V}$ .



a)



b)

Figure 4.3: Bus voltages for different power injections at bus 27 in a) radial case and b) meshed case  $C_2$

Then, currents in the network are calculated with the DG connected at bus 27 injecting  $P_{27}^{Max,V}$ . Since no violation has occurred, the final value for  $P_{27}^{Max,Total}$  is 0.908 MW. When operating the system in the meshed configuration  $C_2$ , the value of  $P_{27}^{Max,V}$  is found to be 2.304 MW using the proposed method, which shows an increase of 199%. If the repetitive power flow method was used, this value was obtained as 2.498 MW. The

voltages of the buses for different values of injected power at bus 27 with unity power factor when the system is operated in meshed configuration  $C_2$  are shown in Figure 4.3b, which verifies the obtained value for the  $P_{27}^{Max,V}$  in this operating scenario. As Figure 4.3 reveals, system voltages are more robust in the meshed configuration  $C_2$  while the injection at bus 27 is increased, and hence are less prone to violate their acceptable limits. This also confirms that the value of  $P_{27}^{Max,V}$  is higher in meshed configuration  $C_2$ .

In the next two sections, the maximum allowable generation of a single DG connected to the system is calculated and compared for different configurations. Two different demand scenarios have been considered as the worst case conditions of the system for calculating the maximum allowable power injection, namely maximum and minimum demand scenarios.

#### 4.3.2 Maximum Demand Scenario

Maximum allowable power injections at different buses in the system for radial and meshed configurations have been estimated using the proposed method. The results for each meshed configuration have been compared with the radial case in the plots shown in Figure 4.4. Results for the buses located at the end of the laterals under different system configurations are shown in Figure 4.5. The following comments can be drawn from these results:

- Each meshed configuration has a different effect on maximum allowable DG injection at different buses in the system. For instance, while meshed configuration  $C_1$  increases this maximum value for bus 59, it reduces the maximum allowable injection at bus 67.

- Variation of the  $P_j^{Max,Total}$  for each bus is different in each configuration: while maximum allowable injection at bus 27 is increased for configuration  $C_2$ , it is decreased for configuration  $C_1$ , and is the same as in the radial case for configuration  $C_5$ .
- The meshed configuration that allows the most amount of power generation is not the same for all buses. For example, the optimum configuration for bus 46 is  $C_5$ , while it is  $C_2$  for bus 65.
- Maximum allowable power injections at some buses are very low. This might be due to the fact that voltages in the system are more sensitive to power injection at these buses. Another reason might be the fact that line current limits near these buses are low, and the DG cannot inject more power to the system, even though bus voltages are not violated. The latter reason, which is more based on the system characteristic and its line current limits, has not happened in the DG unity power factor mode of operation. This will be discussed later, when results under other DG power factors are studied.
- Some buses allow higher power injection in comparison with other buses in the same configuration. Thanks to their location with respect to the substation and the fact that substation voltage is kept constant, these buses have lower voltage sensitivities. However, line current limits might also restrict the maximum allowable power injection at these low-voltage sensitivity buses.
- Figure 4.4 and 4.5 reveal the need for selecting the best meshed configuration, given the desired bus to install the DG at, or selecting the best bus to install



the DG in the specified meshed configuration.

- In all system configurations and assuming unity power factor for the DG, maximum allowable injection at all buses in the system based on voltage limits and DG capacity limit did not violate line current limits. Hence, in this section,  $P_j^{Max,Total}$  was always equal to  $P_j^{Max,V,DG}$ . This might change in different power factors of DG, and will be discussed in Section 4. 4.

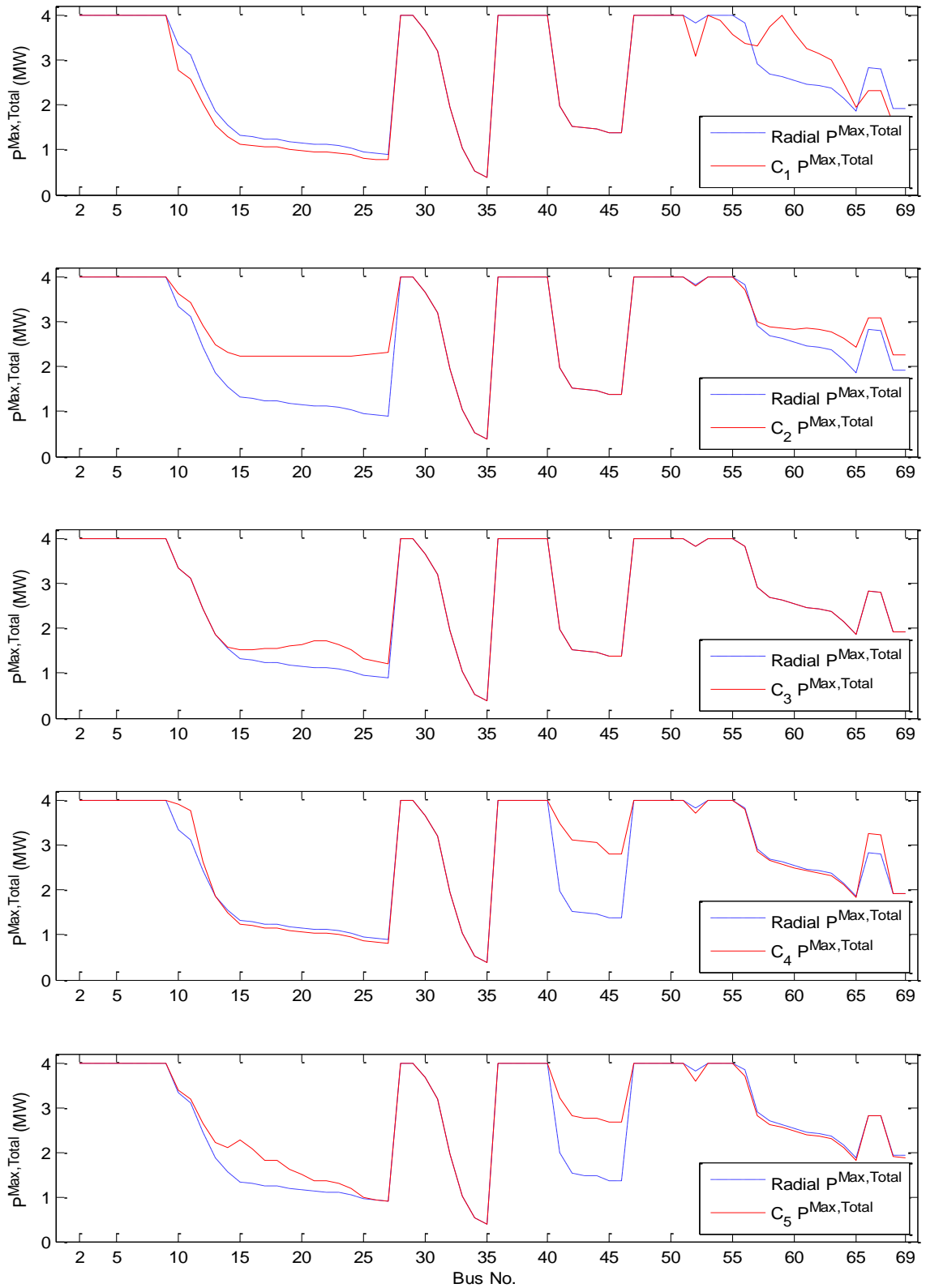


Figure 4.4:  $P^{Max,Total}$  for all system buses in different system configurations, maximum demand scenario and DG unity power factor

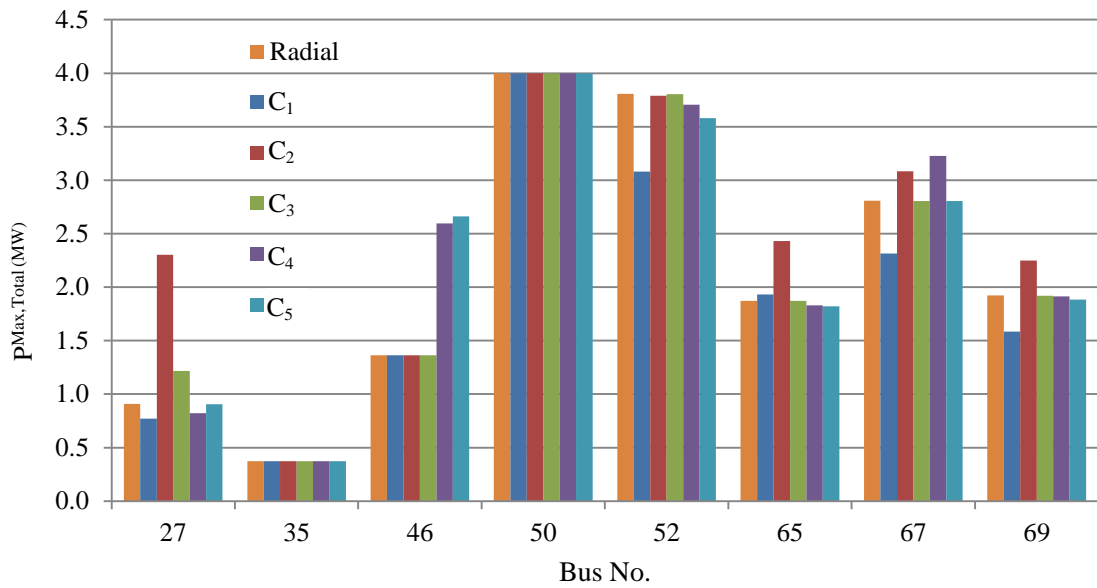


Figure 4.5:  $P^{Max,Total}$  for end-lateral buses in different configurations in maximum demand scenario

#### 4.3.3 Minimum Demand Scenario

Base case (no DG) system voltages for the radial configuration under maximum and minimum demand scenarios are shown in Figure 4.6. As it can be seen in this figure, voltage profile is higher in minimum demand scenario. Hence, system voltages are more prone to overvoltages in low loading conditions, and the minimum demand scenario is expected to have more limitations on the maximum allowable power injection in the system. Maximum allowable DG power injection in unity power factor operation connected at different system buses in radial and meshed configurations is presented in Figure 4.7. This figure also verifies the fact that maximum allowable power injection at a bus varies with changes in system configuration, and each configuration may have different effects on the maximum allowable injection at different buses. In minimum

demand scenario, similar to maximum demand scenario,  $P_j^{Max,Total}$  is equal to

$P_j^{Max,V,DG}$  for all buses when DG power factor is unity.

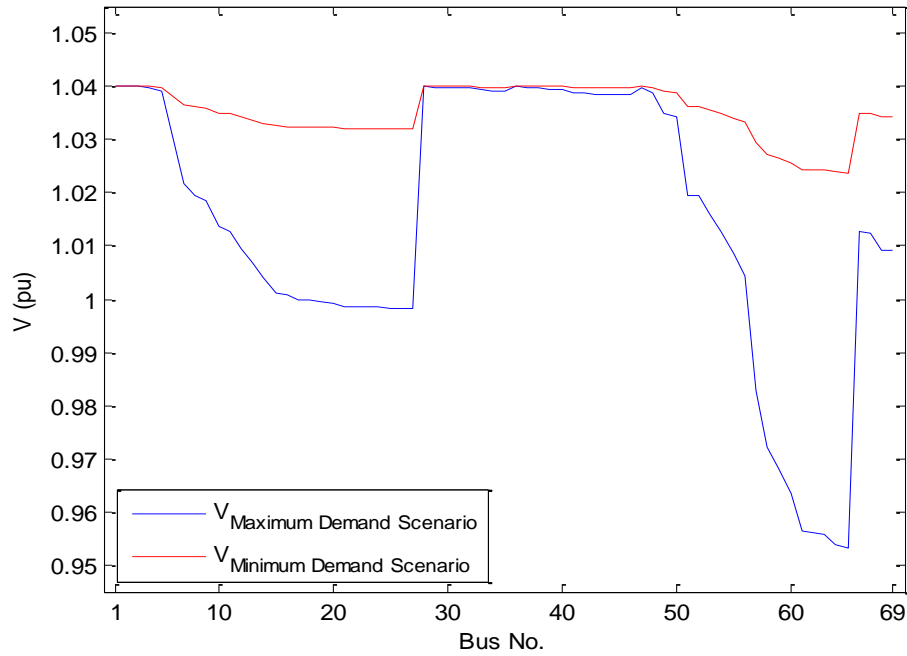


Figure 4.6: System voltage profile for radial configuration without DG in maximum and minimum demand scenario

Figure 4.8 compares the maximum allowable power injection for different buses in the system in maximum and minimum demand scenarios. As can be seen in this figure, for the same system configuration, the minimum demand scenario allows lower maximum power injection in comparison to the maximum demand scenario in the same network configuration. For example, while  $P_{27}^{Max,Total}$  is 2.304 MW in maximum demand scenario and  $C_2$  configuration, its value is 0.752 MW in the same network configuration and minimum demand scenario.

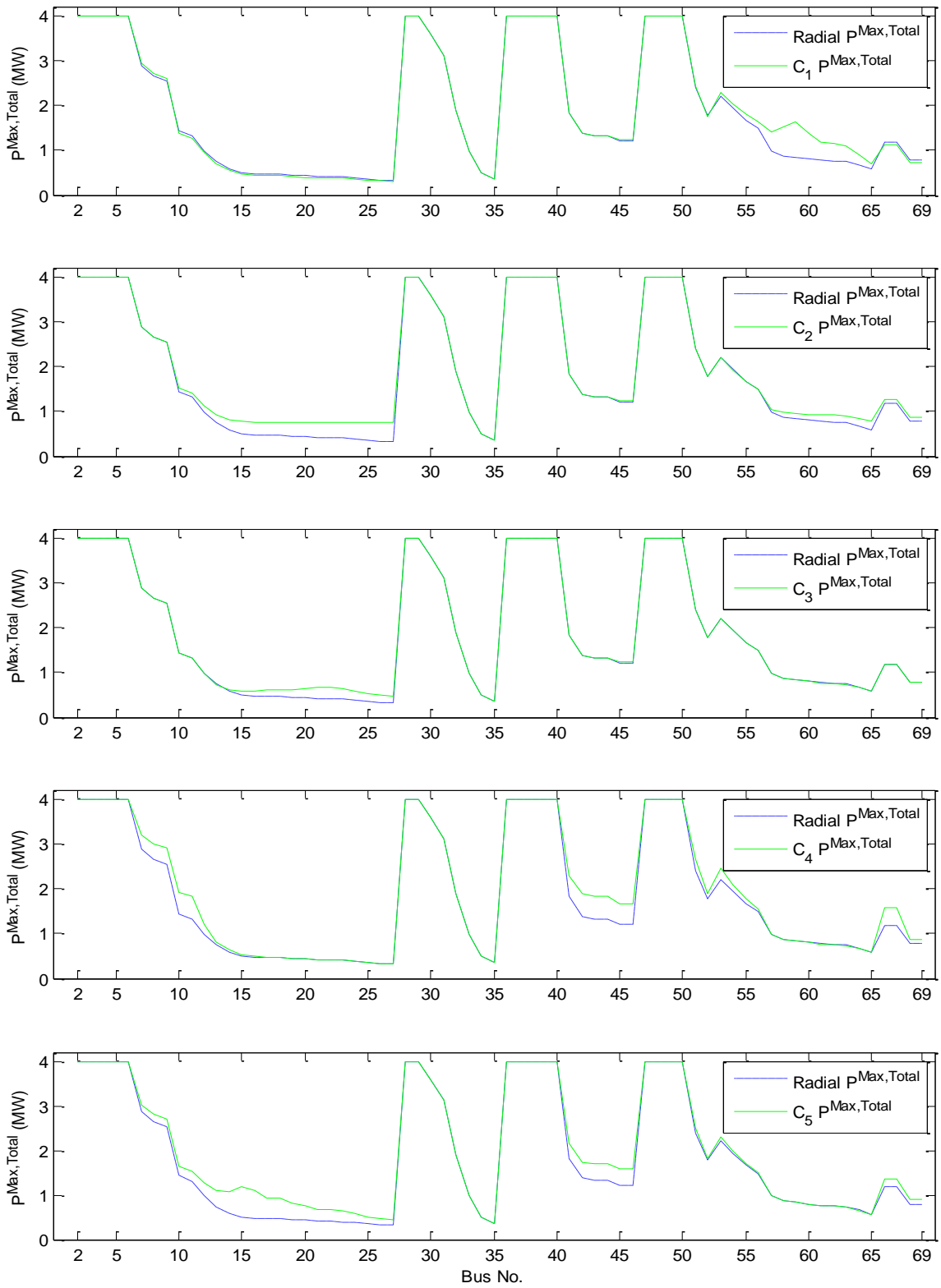


Figure 4.7:  $P^{Max,Total}$  for all system buses in different system configurations, minimum demand scenario and DG unity power factor

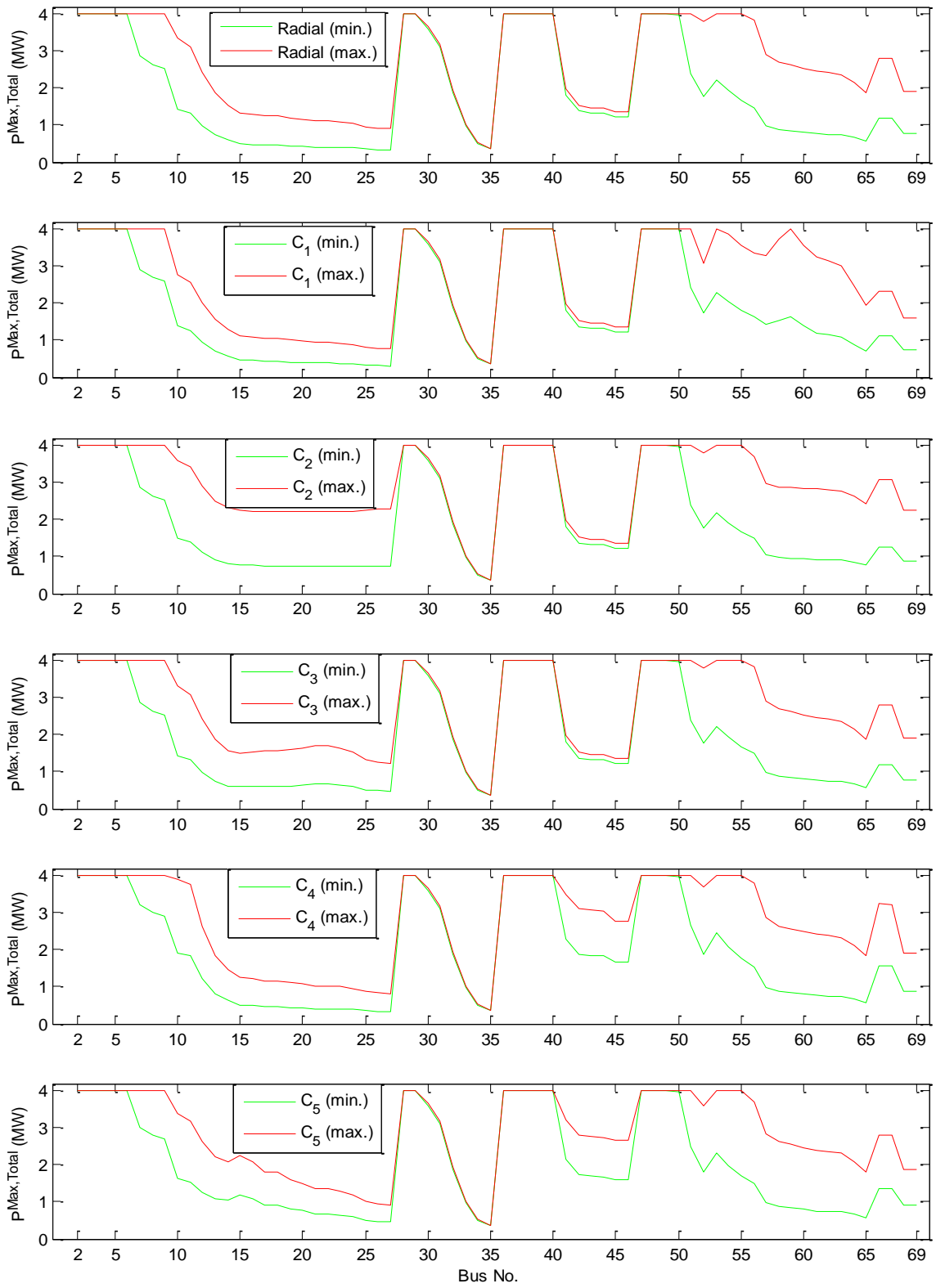


Figure 4.8:  $P^{Max,Total}$  in different system configurations in DG unity power factor in minimum and maximum demand scenarios

#### 4.4 Effect of DG Power Factor

The procedure for obtaining the maximum allowable active power injection is the same for different DG power factors. Changing the DG power factor will not change the system structure; therefore, the values of  $J_{VPQ_{ij}}$  will remain intact in different values of DG power factor. However, in capacitive mode, voltages will be boosted due to the injected reactive power of DG. Therefore, same values of injected active power in capacitive power factors will lead to higher changes in voltages in comparison to unity power factor mode. The maximum allowable penetration levels in system buses due to the voltage limits are expected to be lower than the unity power factor case, since the amount of maximum allowable voltage increase before reaching the upper limit, used in (10), would be less. A similar discussion is also valid for the general trend that the inductive mode of DG operation allows more power injection, since the DG absorbs reactive power and this absorption reduces the voltages. However, this might not always be the case: with increasing the absorbed reactive power, some voltages might violate the lower operating thresholds. It is to be noted that these trends are general expectations and might not be valid for all buses, and the line current limitations will also play a role in the final allowable penetration level.

For simplicity, radial configuration and maximum demand scenario have been considered to see the effect of DG power factor on the maximum allowable DG injection.

Moreover, to see the effect of line current limitations, both  $P_j^{Max,Total}$  and  $P_j^{Max,V,DG}$  have been considered. Figure 4.9 shows these values for all system buses in different plots corresponding to different DG power factors.

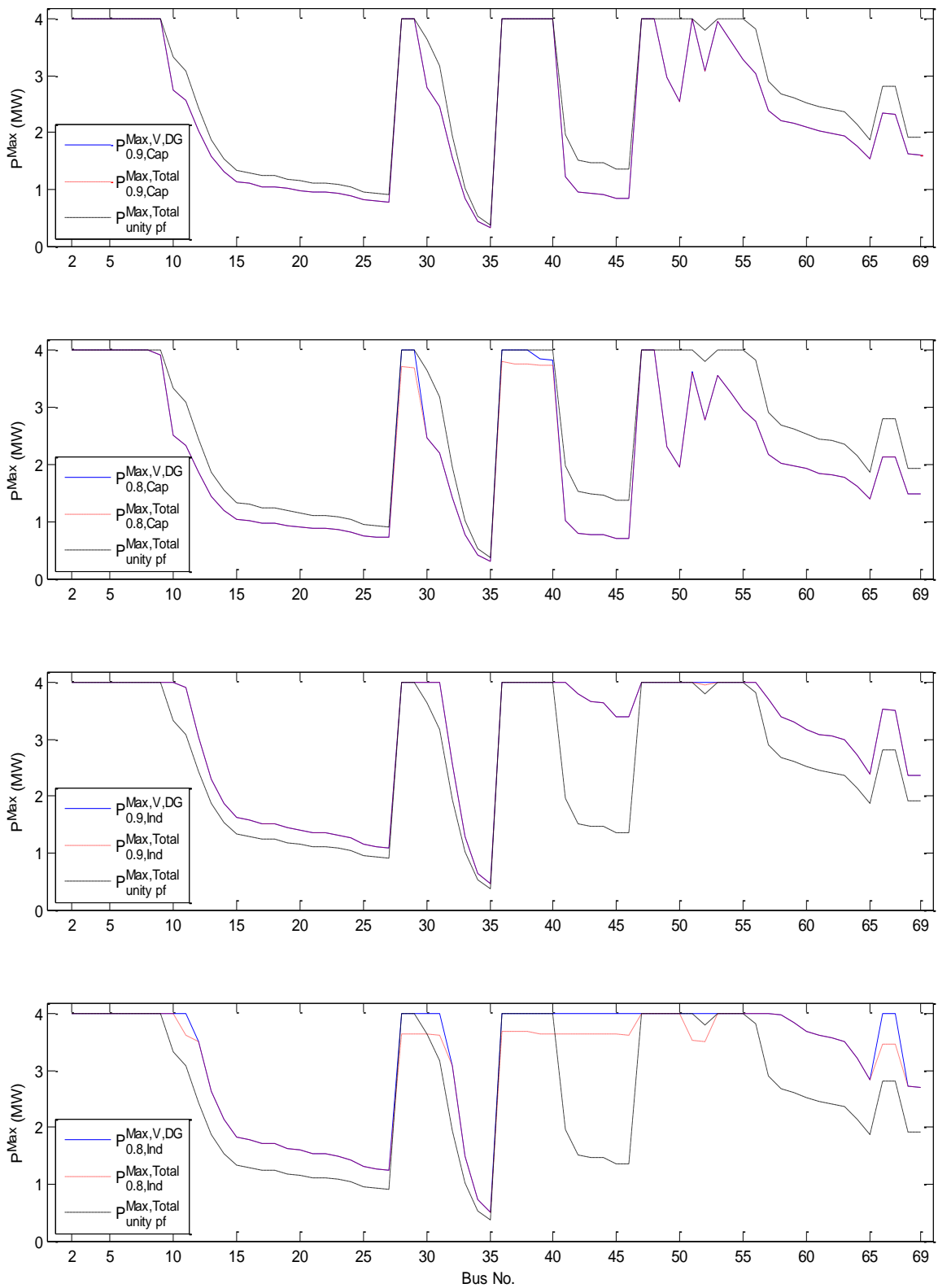


Figure 4.9:  $P^{Max,V,DG}$  and  $P^{Max,Total}$  in radial configuration and maximum demand scenario for different DG power factors



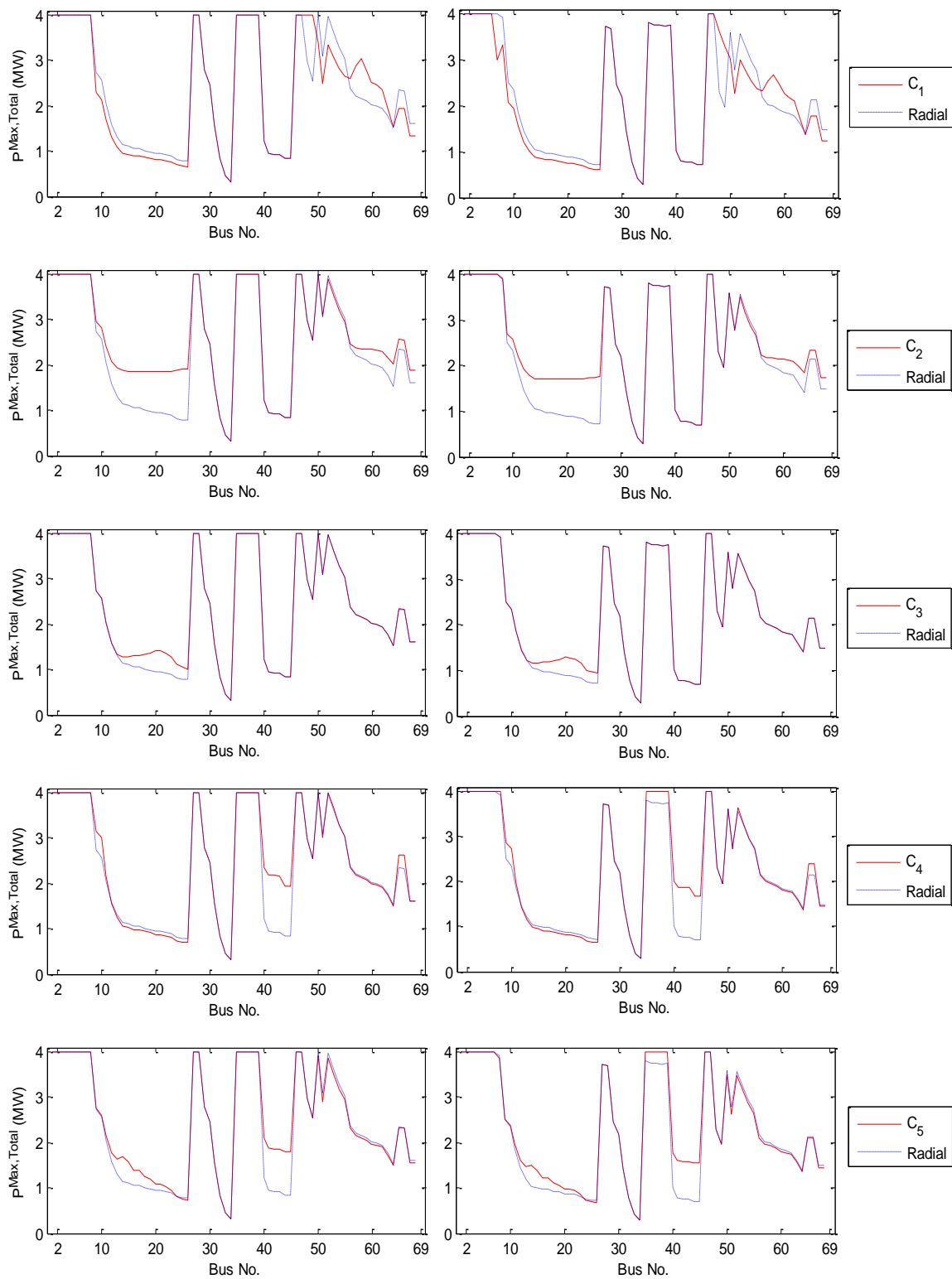
As can be seen in Figure 4.9, moving toward capacitive modes of operating the DG generally decreases the maximum allowable DG power injection. In 0.9 capacitive mode, values of  $P_j^{Max,Total}$  and  $P_j^{Max,V,DG}$  are equal for all buses. Operating the DG with 0.8 capacitive power factor decreases the value of maximum allowable power injection even more. At some buses, like bus 29 and 30, while injecting  $P_j^{Max,V,DG}$  in 0.8 capacitive power factor, the current limits in the system will be violated. Hence, the value of  $P_{29}^{Max,Total}$  is less than  $P_{29}^{Max,V,DG}$ .

In inductive modes of operating the DG, a general trend of increase in the maximum allowable power injection is seen in Figure 4.9. In 0.9 inductive power factor, all buses have higher value of  $P_j^{Max,Total}$  in comparison with the unity power factor. In 0.8 inductive power factor, if the maximum allowable power injection only based on voltage limits and DG capacity is considered, an increase is observable in comparison with the unity power factor. In 0.8 inductive power factor, injecting  $P_j^{Max,V,DG}$  causes the line current to exceed their allowable limits, and hence  $P_j^{Max,Total}$  is less than  $P_j^{Max,V,DG}$ . In some of these buses, the value of  $P_j^{Max,Total}$  in 0.8 inductive power factor is less than its value in unity power factor. For instance,  $P_{52}^{Max,Total}$  in unity power factor is 3.806 MW, while it decreases to 3.510 MW in 0.8 inductive power factor. Bus voltages are not violating their limits in case of injecting 4 MW at bus 52 in 0.8 inductive power factor, i.e.  $P_{52}^{Max,V,DG}$  is 4 MW. However, this power injection also needs a

reactive power absorption of 3 MW, which will cause the line currents to exceed their allowable limits.

Figure 4.10 and Figure 4.11 show the effect of system configuration on maximum allowable DG injection in different DG power factors. As Figure 4.10 demonstrates, although capacitive mode of DG operation decreases the maximum allowable DG power injection, meshed configurations allow more power injection in comparison with radial configuration. A similar conclusion can be made for inductive power factors, as can be seen in Figure 4.11. Meshed configuration might be used to increase the DG injection in comparison with the radial configuration for these power factors as well.

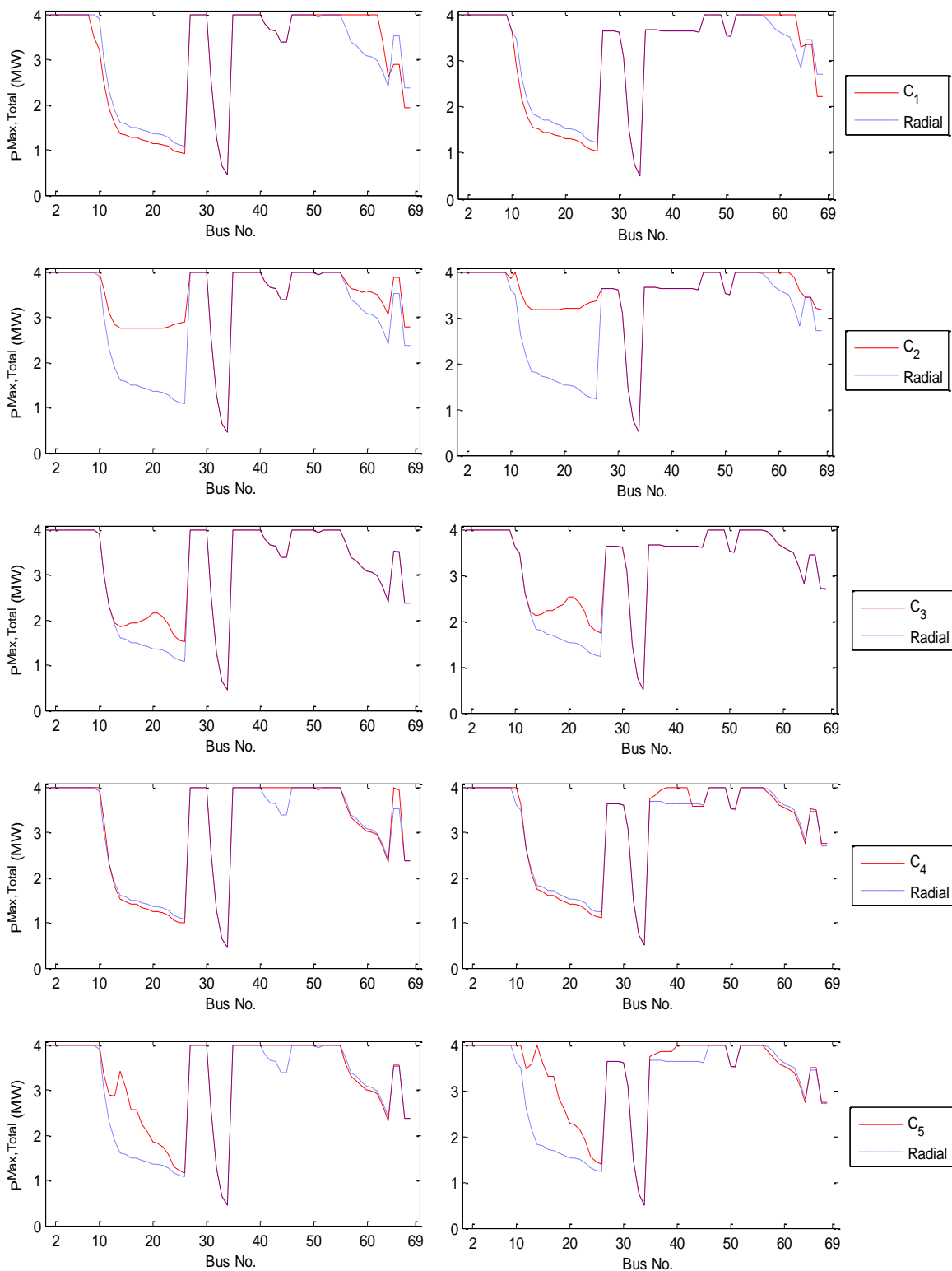
In minimum demand scenario, line currents are typically lower than the maximum demand scenario. The results have shown that the bus voltage limits has a more dominant role in maximum allowable power injection, since in fewer buses the calculated value for  $P_j^{Max,V,DG}$  causes line current limits violations. In general, similar results to the maximum demand scenario are also achieved for the minimum demand scenario, which verify that meshed configurations may allow higher DG injections in the system. For conciseness, these results are not provided here.



a) 0.9 capacitive power factor

b) 0.8 capacitive power factor

Figure 4.10:  $P^{Max.Total}$  in maximum demand scenario for different system configuration in a) 0.9 and b) 0.8 capacitive mode of DG operation



a) 0.9 inductive power factor

b) 0.8 inductive power factor

Figure 4.11:  $P^{Max,Total}$  in maximum demand scenario for different system configurations in a) 0.9 and b) 0.8 inductive mode of DG operation

#### 4.5 Multiple DG Cases: Effect of Radial vs. Meshed Configuration

Thus far in this thesis, the effects of adding one DG at the system have been analyzed. The superior behavior of meshed operation will also be verified in multi-DG scenarios. In these scenarios, the system already has a DG connected to one or more bus/es, and the maximum allowable power injection at another bus is calculated. For simplicity, the unity power factor is considered for the DG units that are being studied in this section, and only maximum demand scenario is considered for the system. The results for values of  $P_j^{Max,Total}$  for end-lateral buses when the system already has a power injection of 1 MW at bus 65 are shown in Table 4.4. The results for radial operation mode are shown in MW, where the results for meshed cases are also shown as percentage increase with respect to the radial case. As can be seen in this table, some conditions allow for significant increase in maximum allowable injected power in comparison to the radial configuration. For example, bus 46 can have more than 85% increase in its power injection with respect to the radial case when 1 MW is injected to the system at bus 65.

This significant feature is also seen when the DG at bus 65 is generating its maximum allowable power in the radial case (1.871 MW). It is to be noted that since the effect of changing the system configuration is to be studied here, the amount of power injection at bus 65 is kept constant although the maximum allowable injection at this bus is different for each configuration. The results of  $P_j^{Max,Total}$  for end-lateral nodes when the DG at bus 65 is operating at 1.871 MW are presented in Table 4.5, which also verifies the advantage of select meshed configurations for increasing DG injection to the system.

Table 4.4: Max. allowable power injection in end-lateral buses in case of having a DG located at bus 65 generating 1 MW

Bus No.	$P_j^{Max,Total}$ (MW)						Inc % in $P_j^{Max,Total}$ with respect to Radial case				
	Radial	$C_1$	$C_2$	$C_3$	$C_4$	$C_5$	$C_1$	$C_2$	$C_3$	$C_4$	$C_5$
27	0.804	0.734	1.521	1.057	0.749	0.849	-8.65	89.18	31.49	-6.80	5.56
35	0.373	0.373	0.373	0.373	0.373	0.373	0.00	0.00	0.00	0.00	0.00
46	1.363	1.363	1.363	1.363	2.576	2.524	0.00	0.00	0.00	89.04	85.21
52	3.117	2.817	3.111	3.115	3.060	2.918	-9.63	-0.17	-0.06	-1.81	-6.39
67	2.369	2.151	2.448	2.366	2.806	2.372	-9.17	3.37	-0.09	18.45	0.14
69	1.644	1.483	1.749	1.642	1.689	1.628	-9.77	6.38	-0.11	2.75	-0.96

Table 4.5: Max. allowable power injection in end-lateral buses in case of having a DG located at bus 65 generating 1.871 MW ( $P_{65}^{Max,Total}$ )

Bus No.	$P_j^{Max,Total}$ (MW)						Inc % in $P_j^{Max,Total}$ with respect to Radial case				
	Radial	$C_1$	$C_2$	$C_3$	$C_4$	$C_5$	$C_1$	$C_2$	$C_3$	$C_4$	$C_5$
27	0.721	0.705	0.801	0.930	0.692	0.803	-2.32	11.00	28.88	-4.06	11.37
35	0.373	0.373	0.373	0.373	0.373	0.373	0.00	0.00	0.00	0.00	0.00
46	1.362	1.362	1.362	1.362	2.415	2.419	0.00	0.00	0.00	77.32	77.54
52	1.760	2.601	2.546	1.757	1.546	1.357	47.84	44.70	-0.16	12.12	-22.90
67	1.646	2.019	1.912	1.644	1.891	1.481	22.62	16.13	-0.16	14.88	-10.06
69	1.423	1.402	1.325	1.421	1.511	1.426	-1.47	-6.87	-0.13	6.19	0.22

As another multi-DG scenario, consider the system with DG at bus 65 generating 1.871 MW in unity power factor, and at bus 27 with 0.69 MW (this is the minimum value in Table 4.5 for all radial and meshed structures when DG at bus 65 is generating 1.871 MW, and has been selected to make the comparison feasible). Table 4.6 shows the results of maximum allowable active power generation in other end-lateral buses in unity power factor in this condition, for different system configurations. As can be perceived from the presented results, the operator can choose the meshed configuration where the allowable generation limit in the specifically desired end-lateral bus is more than other cases. From another perspective, if the configuration is determined, the best bus to have the third DG can be chosen. In any case, results show that if the meshed structure is chosen properly, it generally allows higher penetration levels of DG in the network.

Table 4.6: Max. allowable power injection in end-lateral buses in case of having a DG located at bus 65 and 27, each generating 1.87 MW and 0.69 MW, respectively

Bus No.	$P_j^{Max,Total}$ (MW)						Inc % in $P_j^{Max,Total}$ with respect to Radial case				
	Radial	$C_1$	$C_2$	$C_3$	$C_4$	$C_5$	$C_1$	$C_2$	$C_3$	$C_4$	$C_5$
35	0.373	0.373	0.373	0.373	0.373	0.373	0.00	0.00	0.00	0.00	0.00
46	1.362	1.362	1.362	1.362	0.448	0.609	0.00	0.00	0.00	-67.08	-55.31
52	0.629	0.501	0.694	1.039	0.416	1.118	-20.24	10.41	65.23	-33.83	77.80
67	0.284	0.210	0.429	0.812	0.187	1.119	-26.05	51.41	186.39	-34.22	294.56
69	0.207	0.151	0.345	0.593	0.118	0.811	-27.35	66.72	186.39	-43.02	291.53

#### 4.6 Summary of Results and Observations

In order to compare different system configurations and DG power factors, after calculating the maximum allowable DG penetration for all buses in the system individually, these values are averaged as an index for each “system structure - DG power factor” case. Although the effect of system configuration should be discussed individually for each bus like previous sections, this index can present a general overview of the results. Table 4.7 shows the calculated average among all 68 buses (except the slack bus) of the system in each configuration for maximum demand scenario. The same results are graphically shown in Figure 4.12. As can be seen from these results, the average value for  $P_j^{Max,Total}$  is increased for meshed structures in most cases. The previous discussion on the effect of DG power factor is also verified in this table.

Table 4.7: Average max. allowable power injection in the system for different configurations and DG power factors in maximum demand scenario

	Average $P_j^{Max,Total}$ (MW)				
	Capacitive		Unity	Inductive	
	pf=0.8	pf=0.9		pf=0.9	pf=0.8
Radial	2.152	2.315	2.616	3.050	3.124
$C_1$	2.102	2.281	2.597	3.036	3.086
$C_2$	2.380	2.566	2.926	3.439	3.550
$C_3$	2.205	2.374	2.962	3.154	3.252
$C_4$	2.264	2.422	2.759	3.073	3.135
$C_5$	2.258	2.428	2.799	3.231	3.392



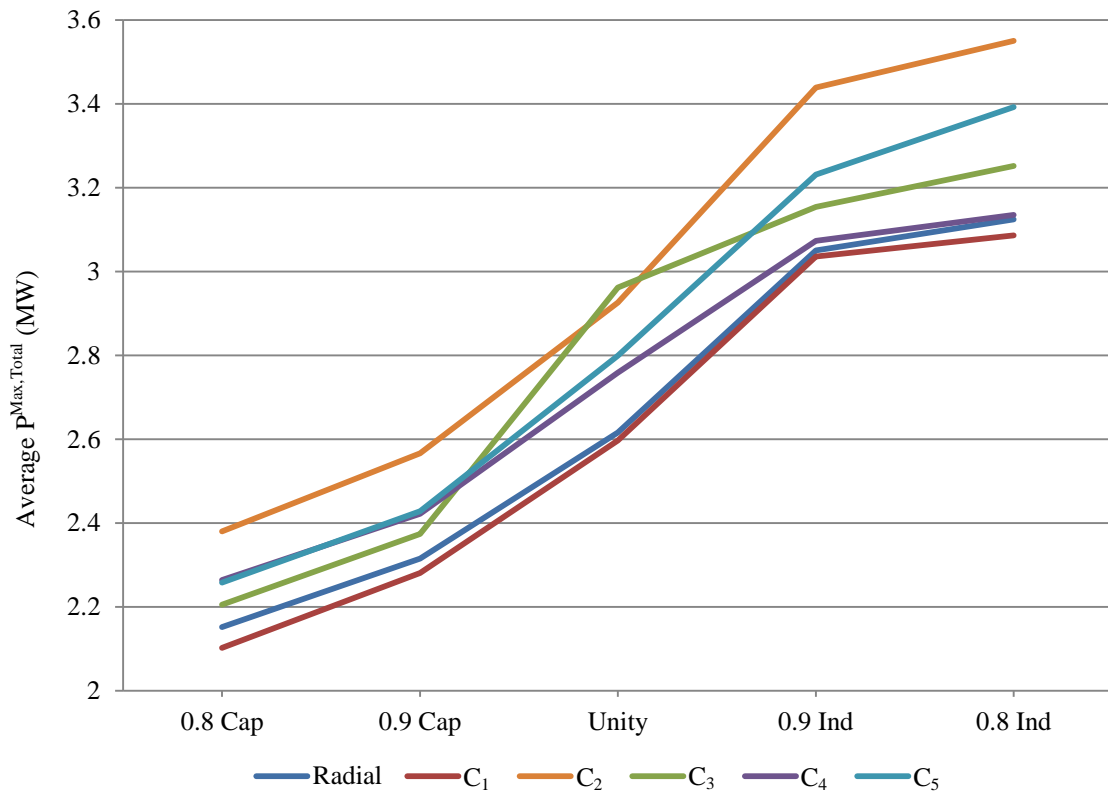


Figure 4.12: Average  $P^{Max,Total}$  (MW) for different configurations and DG power factors in maximum demand scenario

As discussed in Section 1.3, meshed configuration decreases power losses in the system. Table 4.8. shows the active and reactive losses in the system in radial and meshed structures without installing a DG in the system, which verifies the aforementioned advantage of meshed configuration.

Table 4.8: Active and reactive power losses in the system in each configuration

		Configuration					
		Radial	$C_1$	$C_2$	$C_3$	$C_4$	$C_5$
max. demand	$P_{loss}$ (kW)	205.13	105.20	183.41	202.48	185.52	179.24
	$Q_{loss}$ (kVAr)	93.21	75.01	83.22	92.51	86.00	84.92
min. demand	$P_{loss}$ (kW)	7.27	3.97	6.63	7.18	6.62	6.38
	$Q_{loss}$ (kVAr)	3.33	2.84	3.03	3.30	3.10	3.07

## CHAPTER 5: CONCLUSION

### 5.1 Overview

The work in this thesis investigates advantages of selective meshing of electrical distribution systems to allow for higher DG power injection. In this chapter, research contributions and accomplishments of the work are summarized in Section 5.2. Section 5.3 then discusses the future vision.

### 5.2 Summary of Research Contributions

Due to environmental and societal concerns in recent years, the attention toward possible increase in injection levels of Distributed Generation (DG) to the distribution system has drastically increased. The use of DG increases system efficiency providing power closer to the customers, and improves system voltage profile and reliability. However, the traditionally operated distribution system might need some reinforcement to withstand high penetration levels of DG. This might include updates in the protection system and voltage regulators. Among the most important limiting factors to increasing maximum allowable DG power injection are system-steady state bus voltages and line currents, which need to be maintained within their operating limits.

Distribution systems are traditionally operated in a radial configuration. Appropriately placed loops have been shown to report several advantages over the radial configuration. These advantages include reliability increase, voltage profile improvement and power loss reduction. Often, in order to increase their reliability, even radial

distribution systems present normally open tie lines. Therefore, there would be no need for new line construction for the system to be operated in a looped manner. This thesis evaluates the ability of distribution system meshed configuration to allow for higher penetration levels of DG in the system.

For this purpose, a method to determine the maximum allowable DG injection to the system considering steady-state system voltages and line currents is presented in this thesis. The proposed method solves power flow only once; it then uses closed-form equations based on the system Jacobian matrix to determine maximum DG injection. The proposed method is faster and has less computational burden than the repetitive power flow method for determining maximum allowable DG injection. This helps the operator to use this method in a more dynamic way, since the load curve and PV power output are typically changing during a day. The maximum allowable DG injection for a 69-bus test system is compared in different meshed configurations with the radial configuration.

The achieved results show that:

- Meshed configuration of the distribution system generally increases the maximum allowable DG injection.
- The best meshed configuration can be selected to have the highest allowable DG injection at a desired bus.
- Given a meshed configuration, the best location (i.e. bus) for DG interconnection can be selected based on highest allowable DG injection.
- Meshed configuration, if properly chosen, allows for higher DG injection in multi-DG scenarios as well.
- Meshed configuration causes the system power losses to decrease in

comparison to the radial case.

### 5.3 Future Work and Vision

Several suggestions and comments can be made in terms of future vision for the work presented in this thesis. Ideas for additions and improvements to the proposed work include:

- The presented method considers steady-state voltages and currents in the system. Due to their intermittent nature, renewable DG like PV systems might also cause transient over- or under- voltages. Meshed configuration could be also compared with radial configuration with respect to the maximum overshoot of the transient voltages caused by the DG.
- Other elements of the distribution system such as protection system and voltage regulators could be considered in the comparison between meshed and radial configuration. Meshed configuration can be assessed with respect to the updates/ costs required to upgrade these elements. Then, given the long term (5-10 years) benefits of the ability to increase renewable DG in the meshed configuration, a comparison can be made between meshed and radial configurations based on total costs and benefits.
- A Network Reconfiguration (NR) optimization problem with relaxed radiality constraints could be formulated to select the best meshed configuration to maximize the injected power at a desired bus. Constraints of steady-state voltage and current limits, transient voltage limits, cost of upgrading the protection system and voltage regulators, and other possible

factors could be taken into account.

- In this thesis, place of tie-lines which form loops in the system is constant. A switch placement problem, similar to the previous point, could be formulated to select the best place to form the mesh, i.e. the best location of the tie-switch. This could be utilized in designing new distribution systems as well as upgrading the existing systems.

## REFERENCES

- [1] W. H. Kersting, *Distribution System Modeling and Analysis*, 3<sup>rd</sup> Edition, CRC Press, 2012.
- [2] A. J. Pansini, *Electrical Distribution Engineering*, 3rd Edition, The Fairmont Press, 2007.
- [3] J. R. Agüero, “Improving the efficiency of power distribution systems through technical and non-technical losses reduction,” in *Proc. Transmission and Distribution Conference and Exposition (T&D)*, Orlando, FL, May 2012.
- [4] A. Y. Abdelaziz, F. M. Mohamed, S. F. Mekhamer, and M. A. L. Badr, “Distribution system reconfiguration using a modified Tabu search algorithm,” *Electric Power Systems Research*, vol. 80, no. 8, pages 943–953, August 2010.
- [5] J. S. Savier and D. Das, “Impact of network reconfiguration on loss allocation of radial distribution systems,” *IEEE Transactions on Power Delivery*, vol. 22, no. 4, pp. 2473-2480, October 2007.
- [6] C. J. Mozina, “Impact of green power distributed generation,” *IEEE Ind. Appl. Mag.*, vol. 16, no. 4, pp. 55-62, July/August 2010.
- [7] M. H. J. Bollen and F. Hassan, *Integration of Distributed Generation in the Power Systems*, IEEE Press, 2011.
- [8] G. Celli, F. Pilo, G. Pisano, V. Allegranza, R. Cicoria, and A. Iaria, “Meshed vs. radial MV distribution network in presence of large amount of DG,” in *Proc. IEEE Power Energy Soc. Power Syst. Conf. Expo.*, vol. 2, pp. 709-714, October 2004.
- [9] M. Al-Muhaini and G. T. Heydt, “Evaluating future power distribution system reliability including distributed generation,” *IEEE Transactions on Power Delivery*, vol. 28, no. 4, pp. 2264-2272, October 2013.
- [10] C. A. Penuela Meneses and J. R. Sanches Mantovani, “Improving the system operation and reliability cost of distribution systems with dispersed generation,” *IEEE Transactions on Power Systems*, vol. 28, no. 3, pp. 2485-2496, August 2013.
- [11] M. E. H. Golshan and S. A. Arefifar, “Distributed generation, reactive sources and network-configuration planning for power and energy-loss reduction,” *Generation, Transmission and Distribution, IEE Proceedings*, vol. 153, no. 2, pp. 127-136, March 2006.

- [12] D. Q. Hung and N. Mithulananthan, "Multiple distributed generator placement in primary distribution networks for loss reduction," *IEEE Transactions on Industrial Electronics*, vol. 60, no. 4, pp. 1700-1708, April 2013.
- [13] I. K. Song, W. W. Jung, J. Y. Kim, S. Y. Yun, J. H. Choi, and S. J. Ahn, "Operation schemes of smart distribution networks with distributed energy resources for loss reduction and service restoration," *IEEE Transactions on Smart Grid*, vol. 4, no. 1, pp. 367-374, March 2013.
- [14] V. R. Pandi, H. H. Zeineldin, and W. Xiao, "Allowable DG penetration level considering harmonic distortions," *IECON 2011- 37th Annual Conference on IEEE Industrial Electronics*, pp. 814-818, November 2011.
- [15] A. Bhowmik, A. Maitra, S. M. Halpin, and J. E. Schatz, "Determination of allowable penetration levels of distributed generation resources based on harmonic limit considerations," *IEEE Transactions on Power Delivery*, vol. 18, no. 2, pp. 619-624, April 2003.
- [16] A. F. Abdul Kadir, A. Mohamed, and H. Shareef, "Harmonic impact of different distributed generation units on low voltage distribution system," *IEEE International Electric Machines & Drives Conference (IEMDC)*, May 2011.
- [17] V. Khadkikar, R. K. Varma, R. Seethapathy, A. Chandra, and H. Zeineldin, "Impact of distributed generation penetration on system current harmonics considering non-linear loads," *3rd IEEE International Symposium on Power Electronics for Distributed Generation Systems (PEDG)*, June 2012.
- [18] T. H. Chen, W. C. Yang, Y. D. Cai, and N. C. Yang, "Voltage variation analysis of normally closed-loop distribution feeders interconnected with distributed generation," D N Gaonkar (Ed.), ISBN: 978-953-307-046-9, *InTech*, available from: <http://www.intechopen.com/books/distributed-generation/voltage-variation-analysis-of-normally-closed-loop-distribution-feeders-interconnected-with-distribu>
- [19] J. Morren and S. W. H de Haan, "Maximum penetration level of distributed generation without violating voltage limits," *Smart Systems for Distribution, IET-CIRED Seminar*, June 2008.
- [20] M. E. Baran, H. Hooshyar, Z. Shen, J. Gajda, and K. M. M. Huq, "Impact of high penetration residential PV systems on distribution systems," *IEEE Power and Energy Society General Meeting*, San Diego, CA, July 2011.
- [21] S. Eftekharijad, V. Vittal, G.T. Heydt, B. Keel, and J. Loehr, "Impact of increased penetration of photovoltaic generation on power systems," *IEEE Transactions on Power Systems*, vol. 28, no. 2, pp. 893-901, May 2013.



- [22] V. Cecchi, S. Kamalasan, J. Enslin, and M. Miller, "System impacts and mitigation measures for increased PV penetration levels using advanced PV inverter regulation," *Proceedings of the IEEE 2013 Energy Conversion Congress and Exposition (ECCE)*, September 2013.
- [23] P. Pachanapan, A. Dysko, O. Anaya-Lara, and K. L. Lo, "Harmonic mitigation in distribution networks with high penetration of converter-connected DG," *IEEE PowerTech*, June 2011.
- [24] M. Loos, S. Werben, and J. C. Maun, "Circulating currents in closed loop structure, a new problematic in distribution networks," *IEEE Power and Energy Society General Meeting*, July 2012.
- [25] F. A. Viawan, D. Karlsson, A. Sannino, and J. Daalder, "Protection scheme for meshed distribution systems with high penetration of distributed generation," *Power Systems Conference: Advanced Metering, Protection, Control, Communication, and Distributed Resources*, March 2006.
- [26] T. H. Chen, W. T. Huang, J. C. Gu, G. C. Pu, Y. F. Hsu, and T. Y. Guo, "Feasibility study of upgrading primary feeders from radial and open-loop to normally closed-loop arrangement," *IEEE Transactions on Power Systems*, vol. 19, no. 3, pp. 1308-1316, August 2004.
- [27] W. C. Yang, T. Chen, and J. D. Wu, "Effects of renewable distributed generation on the operational characteristics of meshed power distribution systems," *WSEAS Transactions on Power Systems*, vol. 4, no. 4, April 2009.
- [28] D. Kamperis, G. M. A. Vanalme, and W. L. Kling, "The ability of a Dutch LV network to incorporate high penetration level of  $\mu$ -CHPs considering network topology and units control strategy," *2nd IEEE PES International Conference and Exhibition on Innovative Smart System Technologies (ISGT Europe)*, December 2011.
- [29] P. Karimi-Zare and H. Seifi, "Maximum allowable penetration level determination of a DG in a distribution network," *IEEE International Energy Conference and Exhibition (ENERGYCON)*, September 2012.
- [30] H. M. Ayres, W. Freitas, M. C. De Almeida, and L. C. P. da Silva, "Method for determining the maximum allowable penetration level of distributed generation without steady-state voltage violations," *IET Generation, Transmission & Distribution*, vol. 4, no. 4, pp. 495-508, April 2010.
- [31] J. Sadeh, M. Bashir, and E. Kamyab, "Effect of distributed generation capacity on the coordination of protection system of distribution network," *IEEE/PES Transmission and Distribution Conference and Exposition: Latin America (T&D-LA)*, November 2010.

- [32] J. M. Bloemink and T. C. Green, "Increasing photovoltaic penetration with local energy storage and soft normally-open points," *IEEE Power and Energy Society General Meeting*, July 2011.
- [33] H. Saadat, *Power System Analysis*, 3rd ed., PSA Publishing, 2010.
- [34] M. E. Baran and F. F. Wu, "Optimal capacitor placement in distribution systems," *IEEE Transactions on Power Delivery*, vol. 4, no. 1, pp. 725–734, January 1989.
- [35] Y. C. Huang, "Enhanced genetic algorithm-based fuzzy multi-objective approach to distribution network reconfiguration," *Generation, Transmission and Distribution, IEE Proceedings*, vol. 149, no. 5, pp. 615-620, September 2002.